EPRI

Fuel Performance Analysis Capability in FALCON

Technical Report

Fuel Performance Analysis Capability in FALCON

1002866

Final Report, December 2002

EPRI Project Manager
S. Yagnik

EPRI • 3412 Hillview Avenue, Palo Alto, California 94304 • PO Box 10412, Palo Alto, California 94303 • USA
800.313.3774 • 650.855.2121 • askepri@epri.com • www.epri.com

DISCLAIMER OF WARRANTIES AND LIMITATION OF LIABILITIES

THIS DOCUMENT WAS PREPARED BY THE ORGANIZATION(S) NAMED BELOW AS AN ACCOUNT OF WORK SPONSORED OR COSPONSORED BY THE ELECTRIC POWER RESEARCH INSTITUTE, INC. (EPRI). NEITHER EPRI, ANY MEMBER OF EPRI, ANY COSPONSOR, THE ORGANIZATION(S) BELOW, NOR ANY PERSON ACTING ON BEHALF OF ANY OF THEM:

(A) MAKES ANY WARRANTY OR REPRESENTATION WHATSOEVER, EXPRESS OR IMPLIED, (I) WITH RESPECT TO THE USE OF ANY INFORMATION, APPARATUS, METHOD, PROCESS, OR SIMILAR ITEM DISCLOSED IN THIS DOCUMENT, INCLUDING MERCHANTABILITY AND FITNESS FOR A PARTICULAR PURPOSE, OR (II) THAT SUCH USE DOES NOT INFRINGE ON OR INTERFERE WITH PRIVATELY OWNED RIGHTS, INCLUDING ANY PARTY'S INTELLECTUAL PROPERTY, OR (III) THAT THIS DOCUMENT IS SUITABLE TO ANY PARTICULAR USER'S CIRCUMSTANCE; OR

(B) ASSUMES RESPONSIBILITY FOR ANY DAMAGES OR OTHER LIABILITY WHATSOEVER (INCLUDING ANY CONSEQUENTIAL DAMAGES, EVEN IF EPRI OR ANY EPRI REPRESENTATIVE HAS BEEN ADVISED OF THE POSSIBILITY OF SUCH DAMAGES) RESULTING FROM YOUR SELECTION OR USE OF THIS DOCUMENT OR ANY INFORMATION, APPARATUS, METHOD, PROCESS, OR SIMILAR ITEM DISCLOSED IN THIS DOCUMENT.

ORGANIZATION(S) THAT PREPARED THIS DOCUMENT

ANATECH Corp

ORDERING INFORMATION

Requests for copies of this report should be directed to EPRI Orders and Conferences, 1355 Willow Way, Suite 278, Concord, CA 94520, (800) 313-3774, press 2 or internally x5379, (925) 609-9169, (925) 609-1310 (fax).

CITATIONS

This report was prepared by

ANATECH Corp.
5435 Oberlin Drive
San Diego, California 92121

Principal Investigators
W. Lyon
R. Montgomery
A. Zangari
D. Sunderland
Y. Rashid
R. Dunham

This report describes research sponsored by EPRI.

The report is a corporate document that should be cited in the literature in the following manner:

Fuel Performance Analysis Capability in FALCON, EPRI, Palo Alto, CA: 2002. 1002866.

REPORT SUMMARY

The Fuel Analysis and Licensing Code—New (FALCON) is being developed as a state-of-the-art light water reactor (LWR) fuel performance analysis and modeling code validated to high burnup. Based on a robust finite-element numerical structure, it is capable of analyzing both steady-state and transient fuel behaviors with a seamless transition between the two modes. EPRI plans to release a fully benchmarked and validated beta version of FALCON in 2003.

Background

Historically, EPRI has supported two fuel performance codes—ESCORE for steady-state reload analysis and FREY for fuel reliability and off-normal transient analysis. In 1996, EPRI initiated development of FALCON, combining the best features of ESCORE and FREY. This had become necessary for three main reasons. First, ESCORE and FREY worked on different numerical structures and required a cumbersome initialization procedure to analyze a fuel transient after steady-state operation to a certain burnup. Second, ESCORE and FREY predictions were inconsistent with more recent high burnup and high-duty fuel behavior data. Third, many users of ESCORE and FREY continued to express the need for capability enhancements, in particular, the ability to deal with newer cladding materials, mixed oxide (MOX) fuel, and burnable absorbers. FALCON development activities will reach a significant milestone with release of the beta version in 2003.

Objectives

To outline fuel performance analysis capabilities of FALCON and summarize its status prior to beta version release; to develop a reference document that captures FALCON developmental efforts underway since 1996.

Approach

Using the existing experience base from ESCORE and FREY, FALCON developers focused their efforts in three major areas. First, they assimilated a robust numerical scheme with fully coupled thermal and mechanical iterations to perform steady-state and transient analyses seamlessly in a single code. Second, they incorporated pellet and cladding material and behavior models required for steady-state and transient fuel performance analysis, with an emphasis on upgrading these models for high burnup applications, where appropriate. Third, they developed input decks for FALCON benchmarking, verification, and validation based on widely representative cases of test reactor experiments and commercial reactor fuel rods.

Results

Concurrent with development work since 1996, various interim versions of FALCON have been used to support recent industry demands. These include fuel rod design evaluations, analysis of reactivity insertion accident (RIA) tests, development of revised RIA acceptance criteria, analytical support for the Argonne National Laboratory – Nuclear Regulatory Commission Loss of Coolant Accident (ANL-NRC LOCA) Program, and dry storage of high burnup spent fuel. As a result, the beta release version of FALCON has undergone substantial improvements compared to ESCORE and FREY. Benchmarking of the beta version has been initiated and selected results are presented in this report. Further adjustments in the code may be necessary as additional benchmarking is undertaken, especially in areas such as steady-state fission gas release and integral fuel rod performance. Developers anticipate completing these and other remaining tasks by mid-2003.

EPRI Perspective

Fuel behavior during both normal and off-normal operations is a complex interaction of thermal, mechanical, and chemical processes. Under some abnormal operational conditions, these processes can threaten fuel integrity and increase demands for more detailed fuel licensing analyses. For optimum plant operation, the detailed behavior of fuel rods under anticipated high burnup needs to be understood and licensed. As new results emerge from various poolside fuel inspections and hot cell post-irradiation examination programs, an analytical capability is indispensable to understand and interpret the results. In addition, the industry needs a validated code to address current and anticipated regulatory concerns over high burnup fuel operation. EPRI anticipates that FALCON will be the tool to meet such challenges. Accordingly, after completion of the FALCON beta version in 2003, EPRI anticipates the formation of a FALCON Users Group. Depending on subsequent utility guidance, the code may also be submitted for design review to obtain 10 CFR 50 Appendix B quality assurance status and NRC approval.

Keywords

Fuel Performance and Modeling
Finite Element Methods
High Burnup Fuel Behavior
Steady-State Fuel Operation
Fuel Response to Transients
Postulated Accidents

CONTENTS

LIST OF FIGURES

LIST OF TABLES

1
INTRODUCTION

This document presents a summary of the current status and capabilities of the Beta release version of the fuel behavior program FALCON. The Alpha version of the code was released in December 1997 [1]. In July 2001, a rigorous peer review was completed to identify outstanding technical issues and focus code development activities. Recently, a special purpose version of the code, FALCON Beta RIA, was submitted for review at the request of the U. S. Nuclear Regulatory Commission (NRC) [2,3]. FALCON Beta RIA was used in support of the revision of the acceptance criteria for the response of light water reactor (LWR) fuel under reactivity initiated accidents (RIA) [4]. The revised criteria are an integral part of a wider industry effort to extend burnup levels beyond those currently licensed.

The introductory section of this document provides background information that describes the objectives of the FALCON's development and evolution into a fully coupled, steady state and transient analysis code. Section 2 presents a general description of the program, its capabilities, and examples of recent applications of the code as well as those envisioned for the future. Section 3 provides a review of FALCON's solution technique, spatial modeling (finite element) methodology, numerical procedure, and material and physical models. It also addresses FALCON's steady state and transient coupling and its approach for computation of deformation and heat transfer. The fourth section describes the activities underway for benchmarking and verification. Selected results from recent benchmarking analyses are presented. Section 5 will summarize the direction of current and future development activities including physical and behavioral models applicable to high burnup operating regimes, advanced fuels (mixed oxide [MOX] and gadolinia-bearing fuels) and cladding types. References are listed at the end of each section.

Background

Traditionally, fuel performance analyses are conducted in two separate parts, steady state and transient phenomena. The reason for this approach is primarily due to limited computing resources. Although workable, this methodology often places significant restraints on the analysis of important fuel behavioral problems that fall into both regimes. This approach also requires coupling of the two analyses, which may be cumbersome depending upon the compatibility of the codes used and often times introduces additional uncertainty into the overall solution. For example, the codes may not necessarily have the same numerical structures and may require substantial effort to interpolate and transfer variables from one to the other. As an example of this approach, the U. S. Nuclear Regulatory Commission (NRC) has supported the development and currently maintains two fuel performance analysis codes, FRAPCON for steady state analyses and FRAPTRAN for transient analyses [5,6]. Similarly, EPRI has supported two fuel performance codes, ESCORE and FREY, for steady state and transient

analyses, respectively. ESCORE is a finite difference-based, quasi-steady state core reload evaluator that has been licensed by the NRC for batch average burnups up to 50 GWd/MTU (lead rod ~60 GWd/MTU). ESCORE is used to support fuel licensing and design basis evaluations [7]. FREY is a finite element, transient thermal/mechanical fuel analysis program used to evaluate fuel rod response under operational transients, Safety Analysis Report (SAR) Chapter 15 Design Basis Events, and other operational conditions that might lead to fuel failures [8]. Both ESCORE and FREY meet 10CFR50 Appendix B Quality Assurance (QA) requirements. ESCORE was reviewed and approved by the NRC in 1990 and has been used by many utilities [9]. FREY has not been submitted to the NRC for review, but was qualified in a design review in 1991 under a 10CFR50-compliant QA program [10]. To facilitate the use of the two codes, an interface procedure linking the two programs was developed in which ESCORE supplies the initial conditions for FREY, thus providing a one-way passive coupling of the two programs.

FREY, and beginning in the late 1980s in combination with ESCORE, has provided an important capability for fuel performance and behavior analyses and has been used to address numerous issues encountered by the industry over the last two decades. These include analyses of fuel behavior phenomena pertaining to Pellet-Cladding Interaction (PCI), relaxation of operational restrictions (PCIOMRs), Loss of Coolant Accidents (LOCA), crud-induced localized corrosion, and RIA. During the mid 1990s industry interest supported the investigation of secondary hydriding in BWR barrier fuel. This led to the development of a diagnostic tool, DEFECT, which used FREY as its basis [11].

Objective

Over the last several years changes in commercial fuel designs and increased fuel utilization have signaled the need for an update in both steady state and transient analysis capability. Examples of recent fuel design changes include new cladding alloys and heat treatments to reduce cladding corrosion and hydriding, and fuel pellet changes to accommodate the enhancement of fission gas release at high burnup. No comparable improvements in capabilities have been introduced in ESCORE in the last decade [12,13]. Also, important additions to the experimental databases for LWR fuel have been made since ESCORE and FREY were released. Particularly important are new experimental observations at fuel peak nodal burnups above 40 GWd/MTU. More fission gas release data has become available at these high burnups and a new phenomenon called the rim effect was discovered [14]. These and the effects of hydrogen uptake (as a byproduct of corrosion) on cladding mechanical properties have come to the forefront as technical issues in fuel behavior modeling. Most recently interest in these issues has been prompted by the results of RIA experiments and the subsequent concerns raised by the NRC about high burnup operation [15].

In order to satisfy the need for an updated fuel performance and behavior analysis capability, EPRI has undertaken the development of the FALCON computer program. The primary objective is to provide an integrated steady state and transient analysis code that preserves the capabilities of both ESCORE and FREY, while enhancing fuel performance and behavior analysis capabilities beyond those currently available. Specifically, the goals of the development program are to provide a code validated with recent high burnup data that offers:

- Validated applicability to high burnup fuel behavior
- Capability to deal with emerging fuel issues and the behavior of high burnup fuel during postulated accidents, e.g. RIA and LOCA
- Ability to perform reload evaluations and independent checks of fuel vendor's calculations
- Reduced maintenance, QA, and documentation costs
- Unique, integrated, and validated capabilities surpassing those of other programs
- Appeal to a wide user base

By combining steady state and transient capabilities into a single code, FALCON provides the user with the versatility and convenience of dealing with a single program for multiple applications, streamlining fuel performance analysis by eliminating the need for transfer of variables, interpolation, and accommodations of differing numerical structures between separate steady state and transient programs. With the inclusion of advanced thermomechanics in a fully two-dimensional continuum framework, updated material property and behavioral models, and an expanded LWR experimental benchmarking and verification database, FALCON provides a new paradigm in the state-of-the-art fuel behavior programs for licensing and best estimate analyses capable of addressing the extended fuel utilization and higher duty issues facing the LWR industry today.

References

1. "FALCON – Fuel Analysis and Licensing Code, Vol. 1: Summary Report on Development Activities," ANATECH Report ANA-97-0230, December 1997.

2. Montgomery, R.O., Rashid, Y.R., "FALCON BETA-RIA: Fuel Analysis for Reactivity Initiated Accident, Vol. 1: Theoretical and Numerical Bases," ANATECH Report ANA-02-0356, October 2002.

3. Zangari, A.J., Montgomery, R.O., "FALCON BETA-RIA: Fuel Analysis for Reactivity Initiated Accident, Vol. 2: User's Manual," ANATECH Report ANA-02-0357, October 2002.

4. Montgomery, R.O., Waeckel, N., Yang, R., "Topical Report on Reactivity Initiated Accident: Bases for RIA Fuel and Core Coolability Criteria," Final Report, 1002865, EPRI, Palo Alto, CA, June 2002.

5. Berna, G.A., et al., "FRAPCON-3: A Computer Code for the Calculation of Steady-State, Thermal-Mechanical Behavior of Oxide Fuel Rods for High Burnup," NUREG/CR-6534, December 1997.

6. Cunningham, M.E., et al., "FRAPTRAN: A Computer Code for the Transient Analysis of Oxide Fuel Rods," NUREG/CR-6739, Vol. 1, August 2001.

7. Kramman, M.A., Freeburn, H.R., Eds., "ESCORE--The EPRI Steady-State Core Reload Evaluator Code: General Description," EPRI NP-5100, EPRI, Palo Alto, California, February 1987.

8. Rashid, Y.R., Montgomery, R.O., Zangari, A.J., "FREY-01: Fuel Rod Evaluation System, Vol. 1: Theoretical and Numerical Bases," Revision 3, Final Report, EPRI NP-3277, EPRI, Palo Alto, CA, August 1994.

9. USNRC Approval Letter, Thadani to Lehmann, May 23, 1990: Acceptance for Referencing of Licensing Topical Report EPRI-NP-5100, "ESCORE – The EPRI Steady-State Core Reload Evaluator Code: General Description."

10. "FREY-01 Design Review," ANATECH Final Report, ANA-QA-135, February 1994.

11. Montgomery, R.O., Rashid, Y.R., "DEFECT – Defective Fuel Element Code - T, Vol. 1: Theoretical and Numerical Bases," Final Report, TR-107887-V1, EPRI, Palo Alto, CA, August 1997.

12. Fiero, I.B., "SPEAR-GAMMA Functional Specifications," NP-2941, March 1983.

13. "ESCORE II Functional Specifications," EPR-004-S-01 (Q), S. Levy Incorporated, 1991.

14. Sunderland, D.J., Harbottle, J., "Selection of Rods to Re-Evaluate ESCORE I by Use of Discriminating Criteria," Stoller Report to S. Levy for EPRI Project 2061-26, August 1991.

15. Montgomery, R.O., Rashid, Y.R., Ozer, O., "Evaluation of Irradiated Fuel During RIA Simulation Tests," EPRI TR-106387, August 1996.

2
CAPABILITIES

FALCON has been developed as a general purpose fuel rod evaluation system applicable to the analysis of steady state conditions, operational transients, and postulated accidents. Its capabilities have been outlined in detail in the documentation submittals for the Alpha and Beta RIA versions of the code [1,2]. The following sections provide a description of FALCON focusing on the current features and updates of the code beyond those in the Beta RIA version. Along with a general overview of FALCON's analysis capabilities a comparison of these features with other fuel performance codes is presented.

General Description

FALCON is based on the finite element computational method and utilizes a single compatible grid for both the thermal solution and the deformation solution. The fuel rod geometry can be represented as either axisymmetric (R-Z) or plane (R-θ) grids treated as two-dimensional continua. FALCON's finite element library consists of 9-node quadrilateral elements that are used to generate a grid for the fuel and cladding. Fuel-cladding gap and pellet-pellet contact are modeled by 2-node elements that simulate gap thermal conductance, friction-slip, and contact-release properties. The plenum is modeled by 2-node elements with thermal and mechanical properties assigned to represent the plenum spring and the gas mixture. Dished and hollow pellets are considered. Heat transfer from the fuel rod to the coolant is modeled by a closed channel thermal hydraulic model using heat transfer coefficients and critical heat flux correlations similar to those used in the EPRI RETRAN and VIPRE thermal-hydraulic programs [3,4]. In addition, several options exist for the application of the coolant flow model within FALCON. Time and space-dependent heat transfer coefficients as well as cladding surface temperature boundary conditions can be specified, thus extending FALCON's applicability to a wide range of transients and heat transfer regimes beyond those represented by the default thermal hydraulic model.

The thermal and mechanical material models are based on the MATPRO material properties library [5]. Significant changes have been made to several of these models as implemented in FALCON. Descriptions of these changes are included in this report as well as in the previous publications describing the Alpha and Beta RIA release versions of the code. MATPRO is a computer library of subprograms that contains basic thermal and mechanical material properties for uranium dioxide (UO_2) and MOX fuels, Zircaloy cladding, and gas mixtures. For each property, the MATPRO document contains a review and evaluation of the data in the literature, the development of a mathematical model based upon theory and experiment, a listing of the subprogram, and a comparison of the model predictions with data. In FALCON, these properties include elastic and inelastic behavior of the fuel and cladding, strain rate dependent plasticity of the cladding, and fuel cracking, relocation, hot-pressing, densification, and swelling. Table 2-1 is

a list of the specific material properties used in FALCON and the routines in which they are called.

Table 2-1
MATPRO Properties Included in FALCON

Material	**Property**	**Subprogram**
Fuel	Specific Heat Capacity	FCP
	Thermal Conductivity	FTHCON
	Emissivity	FEMISS
	Thermal Expansion	FTHEXP
	Elastic Moduli	FELMOD, FPOIR
	Creep Rate	FCREEP
	Densification	FUDENS
	Swelling	FSWELL
	Fracture Strength	FFRACS
Cladding	Specific Heat Capacity	CCP
	Zircaloy Thermal Conductivity and	CTHCON
	ZrO_2 Thermal Conductivity	ZOTCON
	Zirconium Dioxide Emissivity	ZOEMISS
	Thermal Expansion	CTHEXP
	Elastic Moduli	
	Young's Modulus for Isotropic Cladding	CELMOD
	Shear Modulus for Isotropic Cladding	CSHEAR
	Plastic Deformation Parameters	CKMN
	Cold Work and Irradiation Annealing	CANEAL
	Cladding Mechanical Limits	CMLIMT
	Low and High Temperature Oxidation	CORROS, COBILD (EPSIJ in FALCON)
	Meyer Hardness	CMHARD
Fill Gas	Thermal Conductivity	GTHCON
	Viscosity	GVISCO

A steady state initialization procedure is provided for design basis events that initiate from non-zero power levels and non-zero burnup. Definable initial conditions such as fuel relocation, power, fission gas composition, cold gap axial distribution, and cladding strain distributions form basic input to FALCON.

Model Development

As noted above, MATPRO is the primary source of the material property and behavioral models in FALCON. However, one of the major areas of development for FALCON is upgrading the models used within the code to both reflect more modern modeling techniques and experimental data as well as to model phenomena not available within MATPRO or not previously available in the code. Summaries of several of these updates are included below. A variety of sources are being utilized for these model updates including the use and development of models from EPRI-sponsored experimental programs such as the Nuclear Fuel Industry Research Program (NFIR). One example is the NFIR-III program on the effect of high burnup and hydrogen on Zircaloy

cladding properties. This data has been evaluated and work is underway to utilize it for modification of the MATPRO cladding mechanical properties library [6]. Other sources for model modifications, additions, and improvements include computer programs such as ESCORE, and sources available in the open literature. Given that FREY formed the programming basis of FALCON, duplicating ESCORE's capabilities within the code required the migration of many of the fuel and cladding behavioral models needed for steady state analyses from ESCORE to FALCON. Examples of models incorporated into FALCON from ESCORE include fuel relocation, fuel densification, and cladding steady state creep. A comprehensive list of fuel and cladding thermal, mechanical, and behavioral models indicating the source of each model and its primary dependencies is shown Tables 2-2 and 2-3. Note that categories that list multiple sources in Tables 2-2 and 2-3 indicate options within FALCON to utilize multiple models at the user's discretion.

Table 2-2
Fuel Thermal, Mechanical, and Behavioral Models in FALCON

Model	**Source**	**Primary Dependency**
Specific Heat and Enthalpy	MATPRO	T, O/M Ratio
UO_2 Thermal Conductivity	NFIR Modification	T, Burnup, Gd, ρ, Porosity
PuO_2 Thermal Conductivity	MATPRO	T, ρ, O/M Ratio, Pu, Porosity, Burnup (melt T only)
Gas Thermal Conductivity	MATPRO	T, Gas Species Fractions, Pressure, Gap Width
Emissivity	MATPRO	T
Melting Temperature	EdF/Literature	Burnup
Thermal Expansion	MATPRO	T, PuO_2 Fraction, Molten Fraction
Solid Swelling	MATPRO/New Data[1]	T, Burnup
Densification	ESCORE	T, Burnup
Relocation	ESCORE	Burnup, Power Lever
Pellet Cracking	Smeared Crack	T, E, ε_o, ε_f, σ_y (low temp), Creep Compliance, High Temp Strain Rate-Stress Response
Elastic Modulus & Poisson's Ratio	MATPRO	T, ρ, O/M Ratio, Burnup, PuO_2 Fraction
Creep	MATPRO	T, t, Grain Size, ρ, Fission Rate, O/M Ratio, Stress
Steady State Fission Gas Release	ESCORE, ANS5.4, Forsberg-Massih	T, Burnup, Grain Size
Transient Fission Gas Release	Literature	T, Burnup
UO_2 Grain Growth	ESCORE/Literature	T
Pellet Rim Evolution	Lassmann Model	Local Burnup
Radial Power Distribution	TUBRNP	T, ϕ, Fission, Rate, Pu Species Fractions, Burnup
Fuel-Cladding Bonding	Literature	To Be Determined
Burnable Absorbers	Gd/IFBA/Erbia	TUBRNP
Gap Conductance	Ross-Stoute Mikic-Todreas	T, Surface Roughness, Emissivity, μ, P, K

1 - Solid swelling data under review

Table 2-3
Cladding Thermal, Mechanical, and Behavioral Models in FALCON

Model	**Source**	**Primary Dependency**
Specific Heat and Enthalpy	MATPRO	T, H_2
Thermal Conductivity	MATPRO	T, Burnup, Gd, ρ, Porosity
ZrO_2 Thermal Conductivity	NFIR/MATPRO/PFCC[2]	T
Emissivity	MATPRO	T, Oxide Layer Thickness
Thermal Expansion	MATPRO	T
Zr Irradiation Growth	ESCORE/Literature	Φ
Elastic Modulus & Poisson's Ratio	MATPRO	T, O_2, Φ, Cold Work, Texture
Zr Plastic Deformation	MATPRO modified with NFIR	ε_p, $\dot{\varepsilon}$, T, Cold Work, Φ, O_2, H_2
Annealing	MATPRO	T, ~ΔT, Δt, Φ, Cold Work, ϕ
Zr Mechanical Limits	MATPRO modified with NFIR	T, Cold Work, Φ, O_2, $\dot{\varepsilon}$
Failure	PCI/SCC, Transient Rupture, SED[1]	T, t, σ, ε_{burst}
Thermal and Irradiation Creep	MATPRO/Limbäck/ ESCORE	T, σ, ϕ, Φ, $\dot{\varepsilon}$
Meyer Hardness	MATPRO	T
Low Temperature Oxidation	PFCC[2]	T, Coolant Chemistry, H_2, ϕ
High Temperature Oxidation	Leistikov, Cathcart, Baker-Just	T, Coolant Chemistry, H_2, ϕ

1 – Strain energy density

2 – EPRI PWR Fuel Cladding Corrosion model [7]

The following is a brief summary of several selected fuel and cladding behavioral material models in FALCON that are important for steady state analysis. The models include the pellet cladding gap conductance, the UO_2 thermal conductivity, cladding creep, and irradiation growth. Highlights of the models are discussed along with the improvements added to address high burnup.

Gap Conductance

Heat transfer from the fuel pellet to the cladding is controlled by the fuel-cladding gap conductance. Changes in the gap conductance due to gap closure or fission gas release can have a significant impact on the fuel temperatures during operation. Gap conductance models are

typically composed of three terms: gap gas conductivity, solid contact conductance, and radiation conduction. For the case of an open fuel-cladding gap, the conductance is defined by the thermal conductivity of the gas mixture and the effective gap width. A mixture rule is used to combine the conductivities of the different gas constituents to obtain the overall gas conductivity. The effective gap width is a summation of the mechanical gap, the temperature jump distances, and the surface roughnesses of the fuel and cladding. The temperature jump distances represent the ineffectiveness of energy transfer between the gas mixture and the fuel or cladding wall. This inefficiency is expressed mathematically as an increase in the effective gap width. Solid gap conductance is controlled by the interfacial pressure between the fuel and the cladding. Radiative heat conductance is controlled by the outer fuel surface and inner cladding surface temperatures and the emissivity of each material. This term is small for normal operating conditions. The total fuel-cladding gap conductance is a summation of the three separate terms.

The model in FALCON uses all three terms in the fuel-cladding gap conductance calculation. The open gap model is based on the Ross and Stoute data that has a multiplier on the summation of the surface roughnesses [8]. For closed gap conditions, the gap conductance model by Mikic and Todreas is used which contains both the solid contact and the gas conductances [9]. The Mikic and Todreas model uses the interfacial pressure, the fuel and cladding surface roughnesses, and the temperature jump distances to calculate the closed gap conductance. The radiative conductance is added to both the open gap and the closed gap models.

The FALCON gap conductance model is based on the approach used in FREY [10]. Models and data from the literature are being used for comparison to the FALCON model as part of thermal benchmarking. For example, a recent paper by Gates and White suggested for evaluation during the peer review has noted an apparent dependency of the temperature jump distance on fuel radius and surface heat flux [11]. This is a departure from the approach of traditional temperature jump distance formulations and may be incorporated into FALCON to improve the gap conductance model.

UO_2 Thermal Conductivity

In the Alpha version of FALCON, the UO_2 thermal conductivity modeling approach from FREY was used. This approach includes three options to define the UO_2 thermal conductivity: (1) a constant value specified by the user via input, (2) a user specified correlation provided by a specially written subroutine, or (3) the MATPRO correlation. The MATPRO correlation does not have a burnup dependency, however, the model has been modified to include a burnup reduction factor taken from ESCORE [12]. This factor was derived from fuel centerline thermocouple measurements in Halden as a multiplier on the total thermal conductivity and was applied to both the low-temperature and high temperature expressions from the MATPRO UO_2 thermal conductivity model. For the Beta release version of FALCON, a new fuel thermal conductivity model was developed featuring a more rigorous burnup as well as gadolinia (Gd) dependency. This model is based on an empirical model derived from recent thermal diffusivity measurement experiments sponsored by NFIR [13,14]. The NFIR model was chosen because of its capability to represent both the degradation of thermal conductivity due to burnup effects (irradiation damage and fission products) and the thermal recovery of these effects observed during the temperature cycles that occurred in the thermal diffusivity measurements.

Thermal conductivity is typically modeled as a combination of phonon and electronic conductivities. The general formula for thermal conductivity is given by:

$$K = K_{ph} + K_{el}$$

where the phonon conductivity is:

$$K_{ph} = \frac{1}{A + BT}$$

the electronic conductivity is:

$$K_{el} = Ce^{DT}$$

and A, B, C, and D are constants determined empirically from experimental data.

The predominate mode of heat transfer in fuel rods in the temperature regime of interest is through conduction in the crystal lattice via phonon-phonon collisions. Therefore, the impact of burnup on the thermal conductivity of UO_2 is predominately seen in the constants A and B. Similarly, the effect of alloying additions such as Gd on thermal conductivity is also primarily confined to the phonon conductivity. Because these effects are independent, they are additive. Two terms were added to the phonon conductivity equation to account for the presence of Gd in the fuel lattice and its effect on thermal conductivity. The new form of the phonon conductivity equation then becomes:

$$K_{ph} = \frac{1}{A(Bu) + A'(Gd) + [B(Bu) + B'(Gd)]T}$$

where A´ and B´ are dependent on Gd content.

The constants, A´ and B´, were determined from the Gd-dependent thermal conductivity data available from several sources in the literature using a combination of polynomial and exponential least squares fitting techniques [13,15,16,17,18].

In the application of the model in FALCON, the thermal conductivity is further modified by a temperature dependent porosity correction factor, P_f, which is given by:

$$C = 2.58 - 0.00058T$$

$$P_f = \frac{1 - C(1 - D)}{1 - 0.05C}$$

where T is temperature, C is a temperature dependent constant for UO_2, and D is the ratio of the actual fuel density to the theoretical density.

Initial evaluation of the model indicated that it consistently predicted thermal conductivity values for unirradiated and irradiated UO_2. Figure 2-1 presents fuel centerline temperature results from FALCON comparing the MATPRO and the NFIR fuel thermal conductivity models for a moderately high burnup (~ 50 – 55 GWd/MTU) UO_2 test fuel rod. By incorporating the effect of burnup, the NFIR thermal conductivity model provides a much more accurate result when compared to the experimental data than the modified MATPRO model previously used in FALCON.

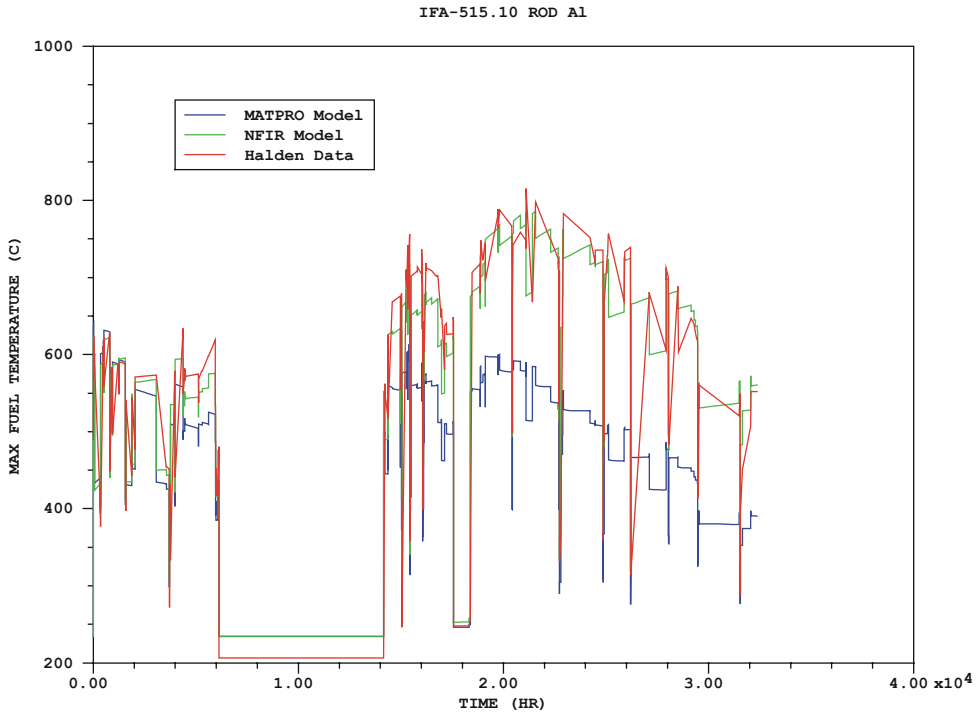

Figure 2-1
Comparison of Maximum Fuel Centerline Temperature as a Function of Irradiation Time for IFA 515.10, Rod A1 (He-Filled Rod) for the MATPRO and NFIR Fuel Thermal Conductivity Models

Testing of the model also indicated the it worked well for unirradiated $(U,Gd)O_2$. However, it consistently under predicted the thermal conductivity for irradiated $(U,Gd)O_2$ samples, indicating that the degradation of irradiated thermal conductivity due to Gd is not as strong as for unirradiated materials. Evaluation of the limited irradiated data available indicated that the reduction in degradation appeared to be proportional to the burnup value. A Gd reduction factor was defined as a function of burnup using data from irradiated $(U,Gd)O_2$ samples and was incorporated into the model. Preliminary tests indicated that it improved the performance of the model for irradiated $(U,Gd)O_2$ rods. Additional testing is planned as part of thermal benchmarking and modifications will likely be made to further refine the model.

Fission Gas Release

In earlier versions of FALCON, steady state fission gas release calculations were based on two primary models: MATPRO FGASRL and the ANS-5.4 model [1,19]. Additionally, options for the use of a user-defined fission gas release model and defined fission gas molar concentrations and percent release were available. When specified as input, the fission gas molar concentrations are defined as volumetric distributions (moles/cm^3) within the fuel grains and on the fuel grain boundaries as functions of both axial and radial position. Along with the specified percent release, this data is used to determine the fuel-cladding gap fission gas molar concentrations to initiate transient calculations. During transients, the EPRI/CE model from FREY is used to determine the grain boundary gas release from the fuel [20]. This model was developed from out-of-pile annealing tests of low burnup fuel. Future model development work will include upgrading the transient fission gas release model employed in FALCON to consider rapid transients and for high burnup applications.

Several additional steady state fission gas release models have been added to the FALCON Beta version release. These are the ESCORE, Forsberg and Massih, and Turnbull fission gas release models [21,22,23]. Summaries of the MATPRO FGASRL, ANS-5.4, and the transient EPRI/CE models are available in the FALCON Beta RIA theory manual. The following paragraphs provide brief summaries of the ESCORE, Forsberg and Massih, and Turnbull fission gas release models.

The ESCORE fission gas release model is characterized by two direct and two indirect gas release mechanisms and computes the amount of fission gas generated and released from the fuel matrix and retained within the grain and grain boundary regions. It also includes a fuel grain growth model based on time, temperature, and initial grain size. An important element of the ESCORE model is gas release by grain boundary sweeping. The direct, athermal release mechanisms are high-energy knockout and recoil and release due to grain boundary sweeping. Indirect release is based on a two-step, time-dependent, diffusional release: first from the fuel matrix to the grain boundaries, and second from the grain boundaries to open porosity leading to release into the fuel-cladding gap.

Recently, a modification was made to the athermal fission gas release component in the ESCORE model as implemented in FALCON. Originally, direct release by knockout and recoil processes was limited to a constant value of 0.2% irrespective of temperature or burnup. A recent paper by Bernard et al. noted an effect on athermal release from an increase in the specific fuel surface at high burnups in the pellet rim region [24]. A modification was introduced into the ESCORE fission gas release model to accommodate this effect. Testing of this change indicated an improvement in the fission gas release predictions using the ESCORE model for low temperature, high burnup rods.

Similar to the ANS 5.4 model, the Forsberg and Massih model is a two-stage fission gas release model based on spherical diffusion from a fuel grain. However, in contrast to previous models, it incorporates time dependent boundary conditions affecting grain boundary gas accumulation, resolution, saturation, and release parameters. Release from the grain boundaries is controlled using a grain boundary saturation criterion. These characteristics also allow the model to accommodate rapid fission gas release from the grain boundaries during power ramps. Forsberg

and Massih also simplified the solution of their time dependent diffusional model by utilizing a solution technique that replaced the kernel of the gas balance equations with a series of exponentials, thus reducing computational complexity.

The Forsberg and Massih model has been implemented and tested at the subroutine level in FALCON. A limited number of evaluations were also conducted during benchmark, verification, and validation case development. The results from these preliminary tests and evaluations have been encouraging, however, additional work is needed to calibrate the model as implemented. The primary focus of the second phase of FALCON benchmarking is fission gas release. Extensive testing and evaluation of the Forsberg and Massih model will be conducted during this phase of the development program.

An additional fission gas release model provided by Turnbull has been implemented in FALCON. This is a highly simplified fuel grain based diffusion model designed to provide a baseline of comparison for evaluation of fission gas release models. It is also used as a test bed to determine the sensitivity of fission gas release modeling parameters such as the diffusion coefficient and grain boundary gas resolution parameter.

Thermal and Irradiation-Induced Cladding Creep

Cladding diametral creep during normal operation and operational transients influences the pellet-cladding gap thickness and pellet-cladding mechanical interaction (PCMI) contact force. Since these have a direct impact on fuel pellet temperatures, cladding creep is an important mechanism to include in a fuel performance modeling code. In the FALCON Beta release, several cladding creep models are available for normal operating temperature conditions (< 450°C). In earlier versions of FALCON, Zircaloy cladding creep was computed using the MATPRO Revision 0 model [5]. The models added to the FALCON Beta release version are the ESCORE, a modified MATPRO Revision 2, and the Limbäck and Andersson cladding creep models [21,25,26]. Each of these models includes both irradiation and thermal creep rate components based on in-pile and out-of-pile creep tests on Zircaloy cladding material.

The general approach used in FALCON is to compute the cladding creep rate using two terms, irradiation-induced creep and thermal creep. The total cladding creep rate is then the sum of the contributions from these two components. The thermal creep rate is further broken down into primary and secondary creep rate components. For normal operating conditions, the cladding diametral creep down process is controlled by irradiation-induced creep deformations. Thermal creep is the controlling creep process that causes stress relaxation and cladding deformations for operational transients that result in PCMI. Under spent fuel storage conditions, the neutron flux is negligible and thermal creep is the dominant cladding creep process. The models used in FALCON for the diametral creep of Zircaloy cladding are dependent on the time, temperature, stress, and fast-neutron flux. Each model also includes a dependence on the material metallurgical condition.

The objective of including the ESCORE, MATPRO Revision 2 and Limbäck and Andersson models is to improve the cladding creep rate model in FALCON through a more robust treatment of the irradiation-induced and thermal creep mechanisms as a function of material metallurgical type and condition. No one model is able to accurately represent all cladding creep conditions.

Each of these models has been included into FALCON to allow for the user to select the model that best suits the needs of the desired analysis.

The ESCORE cladding creep rate model includes two separate terms: irradiation-induced creep and thermal creep. The ESCORE irradiation-induced cladding creep rate component is based on the approach developed by Franklin in the early 1980's [27]. The model coefficients were obtained from a regression analysis of creep data from both fueled and non-fueled rods irradiated in PWR and BWR conditions [28]. The cladding stresses were compressive for the irradiated data. The irradiation-induced creep rate term is added to a thermal cladding creep rate component developed from out-of-pile thermal creep tests with samples subjected to tensile and compressive stresses. The material condition is treated in ESCORE by the use of the unirradiated cladding yield stress at room temperature and the radial texture angle. The ESCORE model was added primarily to serve as a basis of comparison for the evaluation of the newer MATPRO Revision 2 and Limbäck and Andersson cladding creep models and to preserve the ESCORE computational capability within FALCON. The ESCORE model has been applied extensively to operating fuel rod conditions up to 40 GWd/MTU and has been shown to reproduce well cladding creep down strains for commercial fuel rods.

The MATPRO Revision 2 cladding creep model was developed primarily to address irradiation-induced cladding creep down and is based on data from the HOBBIE-1 tests conducted jointly by the US NRC and Engergieonderzoek Centrum Nederland (ECN) [29]. In the tests conducted in the High Flux Reactor at Petten, measurements were made of the in-pile creep down displacements as a function position and time during irradiation. Using this data, the MATPRO Revision 2 model was developed as a function of temperature, fast neutron flux, and compressive hoop stress. The MATPRO Revision 2 model does not depend on the material metallurgical condition of the cladding. Also, the model does not include an explicit thermal creep term. Although the model represents well the data from the HOBBIE-1 experiment, the MATPRO Revision 2 model has not been extensively compared to creep down data from commercial fuel rods.

The Limbäck and Andersson model has recently been developed to represent the effects of metallurgical condition on both the in-pile and out-of-pile creep behavior of Zircaloy cladding. This model includes three key elements: a thermal creep rate expression based on the Matsuo formulation [30], an irradiation hardening effect on the thermal creep rate, and an irradiation-induced creep rate expression based on the model of Hoppe [31]. The out-of-pile thermal creep tests used to develop the model included both cold work stress relieved (CWSR) Zircaloy-4 (Zr-4) and both partially recrystallized annealed (PRXA) and recrystallized annealed (RXA) Zircaloy-2 (Zr-2) cladding material. As a consequence of using this wide array of material, the model coefficients in the Limbäck and Andersson model depend on the metallurgical condition of the cladding. Further, the Franklin data for in-pile creep of CWSR and RXA cladding material was used to develop the model coefficients for the irradiation-induced creep rate expression [27].

The general form of the Limbäck and Andersson model is attractive because the model contains a thermal creep rate model that represents both primary and secondary creep rates, as well as, an irradiation hardening effect on the thermal creep rate that results in irradiation history dependency. These elements of the model are important for calculating the stress relaxation and cladding creep out response during PCMI and cladding creep out deformation during dry storage of spent fuel.

As part of the creep model implementation activities, an evaluation of the MATPRO Revision 0, ESCORE, MATPRO Revision 2, and Limbäck and Andersson creep models was conducted. This evaluation utilized several in-reactor and out-of-pile creep tests representing stress relieved annealed (SRA) and RXA Zr-4 cladding under various temperature, stress, and irradiation conditions. Tables 2-4 and 2-5 provide a list of the data sets used in this evaluation and a description of their testing environments for in-reactor and out-of-pile creep tests, respectively.

Table 2-4
In-Reactor Cladding Creep Test Data

Oconee: SRA and RXA Zr-4 [32]	
SRA S1	103 MPa, 86 MPa, 69 MPa, 340°C, 3270 hrs
SRA V1 and V2	86 MPa, 69 MPa, 340°C, 2960 hrs
RXA S2	103 MPa, 86 MPa, 340°C, 3330 hrs
Gilbon: SRA and RXA Zr-4, M4, and RXA M5 [33]	
SRA Zr-4	90 MPa, 350°C, 6940 hrs
RXA Zr-4	90 MPa, 350°C, 6940 hrs
Halden IFA 585: RXA Zr-2 and SRA Zr-4 [34]	
SRA Zr-4	10 MPa – 12.6 MPa, variable, 375-380°C, up to 2200 hrs

Table 2-5
Out-of-Pile Cladding Creep Test Data

Matsuo: SRA Zr-4 [35]	
SRA	Variable stresses from -117 MPa to 197 MPa including reversals, 360-390°C, up to 3500 hrs
Bouffioux: SRA Zr-4 [36]	
SRA	140, 200, 386 MPa, 650 and 400°C, up to 250 hrs

The results from the evaluation of the in-reactor and out-of-pile creep test data indicated that the MATPRO Revision 2 creep model performed the best overall for tests conducted at temperatures above 340°C for both irradiated and unirradiated data sets. However, it appeared to greatly overestimate the creep strain at temperatures below 340°C, specifically in the irradiation creep term. This prompted a review and a recalibration of the lower temperature fluence dependency in the model. This modification resulted in an improvement in the results from the MATPRO Revision 2 model for irradiation-induced creep.

Because the MATPRO Revision 2 model does not consider the metallurgical condition of the cladding material, a cold work dependency was also introduced into the model using the available data sets of SRA cladding with varying degrees of cold work and fully RXA cladding.

The model was calibrated using the Zr-4 data from Gilbon and tested against the Oconee data. Cold work values for the Oconee SRA samples were determined using room temperature yield stress data. Figures 2-2 through 2-5 show comparisons of results from the modified MATPRO Revision 2 creep model compared to the other models available in FALCON.

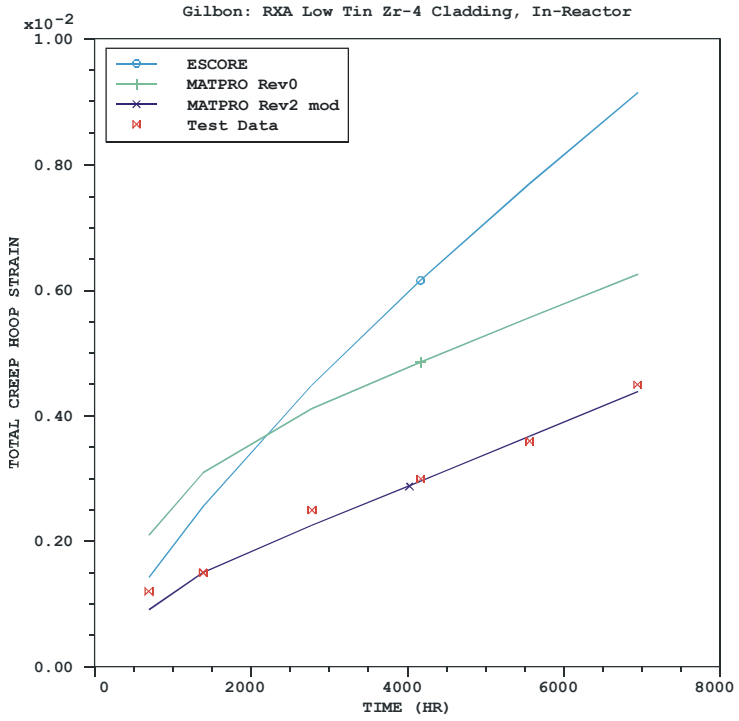

Figure 2-2
Comparison of Total Creep Hoop Strain for Irradiated RXA Zr-4 Cladding

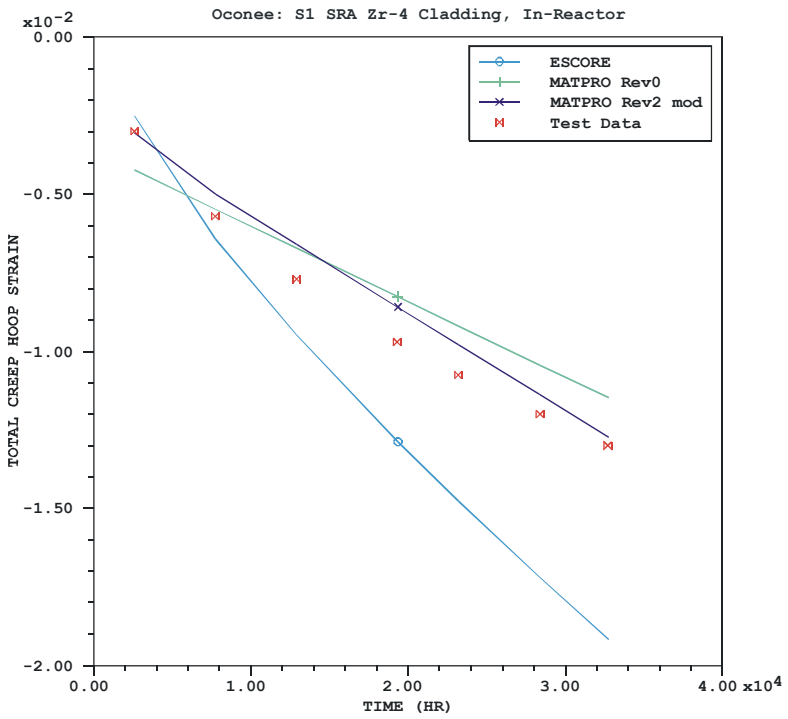

Figure 2-3
Comparison of Total Creep Hoop Strain for Irradiated SRA Zr-4 Cladding

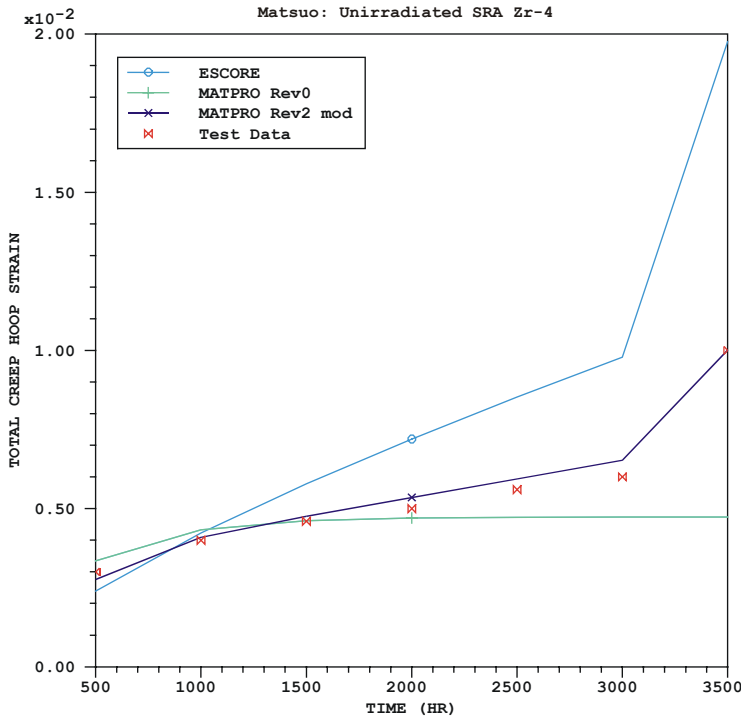

Figure 2-4
Comparison of Total Creep Hoop Strain for Unirradiated SRA Zr-4 Cladding

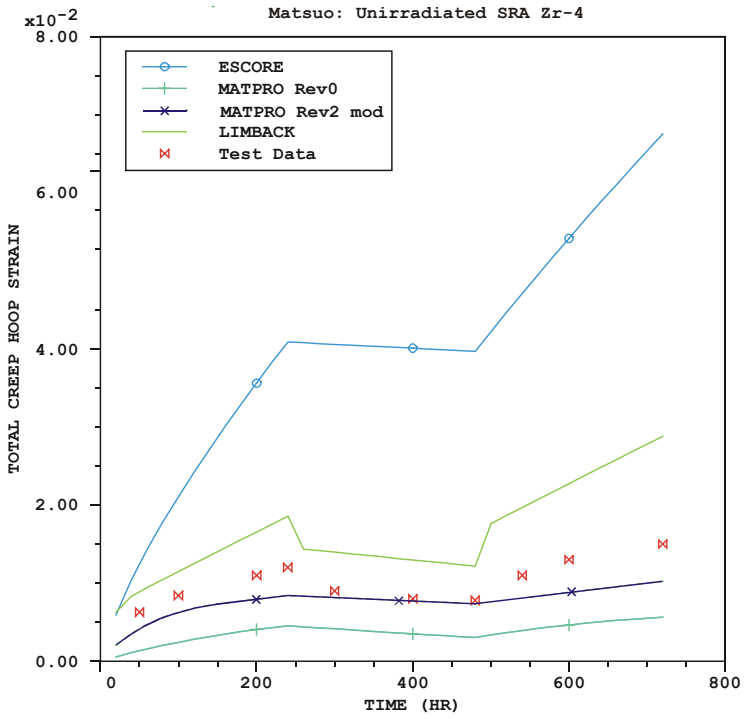

Figure 2-5
Comparison of Total Creep Hoop Strain for Unirradiated SRA Zr-4 Cladding

Figure 2-2 presents data from irradiated creep experiments conducted in the Siloé metallurgical test reactor and computed results from the ESCORE, MATPRO Revision 0, and modified MATPRO Revision 2 creep models for RXA Zr-4 cladding. This data was used to calibrate the modified MATPRO Revision 2 model accounting for cladding metallurgical condition (cold work). As seen in the plot, the modified MATPRO Revision 2 model predicts the response of the RXA Zr-4 (cold work = 0) test data well, whereas both the ESCORE and MATPRO Revision 0 models over predict the measured creep strain (indicating an insensitivity to cladding cold work). Figure 2-3 presents data from irradiated cladding creep tests conducted in Oconee. The test sample shown in this plot is SRA Zr-4 cladding with a cold work of ~ 0.7. Again, the modified MATPRO Revision 2 model represents the test data well, indicating its ability to account for cladding metallurgical condition using cold work.

Figures 2-4 and 2-5 present data from unirradiated SRA Zr-4 cladding tests performed by Matsuo. These tests were preformed under a variety of testing conditions including stress increases, reductions, and reversals as well as temperature increases and reductions. Figure 2-4 illustrates creep strain response during a 30°C temperature increase (at 3000 hrs.) at constant stress. The computed stresses plotted indicate that again the modified MATPRO Revision 2 model represents the test data well. Figure 2-5 presents data and computed results for a stress reversal test of unirradiated SRA Zr-4 cladding. The important finding from this test is that after the stress reversal (at ~ 240 hrs.) the material deforms as if it is not hardened at all indicating that the effect of strain hardening is lost during the stress reversal [35]. Although the modified MATPRO Revision 2 model computed strains are close to the experimental data, the ability to accommodate the lost strain hardening during the stress reversal is available only in the Limbäck

and Andersson model. Both models have been implemented in FALCON and will undergo additional testing during benchmarking and V&V for the Beta version release.

Cladding Irradiation Growth

In the Alpha version of FALCON, axial growth of the cladding was only calculated from Zircaloy thermal expansion and pellet-cladding mechanical interaction effects. No consideration was given to irradiation-induced growth. Such an approach is appropriate for transient events that have a small change in fast fluence. However, irradiation-induced cladding axial growth is important for fuel rod steady state analyses. Post-irradiation examinations often include fuel rod length measurements, which are used to develop the empirical models. This data is useful for code validation and the calculation of fuel rod irradiation growth is required for fuel rod design analysis.

Two cladding irradiation growth models have been incorporated into the Beta release of FALCON and each model can be selected for use via input. These models include the empirical correlation from ESCORE (three variants depending on cladding material type) and the Franklin empirical model for Zr-4 cladding. A user-defined model is also available which allows for the representation of newer cladding alloys or testing of a new/improved irradiation growth model.

In FALCON, the irradiation growth of zirconium alloy cladding is represented by the following empirical equation:

$$\frac{\Delta L}{L} = A(\phi t)^n$$

where

$\frac{\Delta L}{L}$ is the axial strain by irradiation growth

ϕ is the neutron flux (E > 1 MeV)

t is the irradiation time

A,n are empirical model coefficients dependent upon metallurgical condition

Table 2-6 lists the model coefficients for the ESCORE and Franklin Zircaloy cladding irradiation growth models [21,27]. A total of three different cladding material types are represented in the ESCORE model. Differentiation of the ESCORE coefficients is based on the fuel rod vendor identification. The first two cladding variants represent CWSR cladding material. The third set of coefficients for the ESCORE model represents RXA cladding material. The Franklin model was primary developed for CWSR Zr-4 cladding material [27]. For application to RXA material, recently Lanning and Beyer have suggested a modification to the Franklin model. They found that decreasing the A coefficient by a factor of two resulted in better agreement for BWR Zircaloy-2 RXA material [37].

Table 2-6
Cladding Irradiation Growth Model Coefficients Used in FALCON

Model	A (per n/cm^2)	n
ESCORE		
C-E, Exxon, W	3.0×10^{-20}	0.794
B&W	7.35×10^{-25}	1.00
GE	1.82×10^{-15}	0.564
Franklin		
Zr-4 (or CWSR)	2.18×10^{-21}	0.845
Zr-2 (or RXA)	1.09×10^{-21}	0.845

A comparison of the Franklin Zr-4 irradiation growth model to fuel rod length measurements is shown in Figure 2-6. Good agreement with the post-irradiation examination data is found up to fast fluence levels of 1.2×10^{22} n/cm^2.

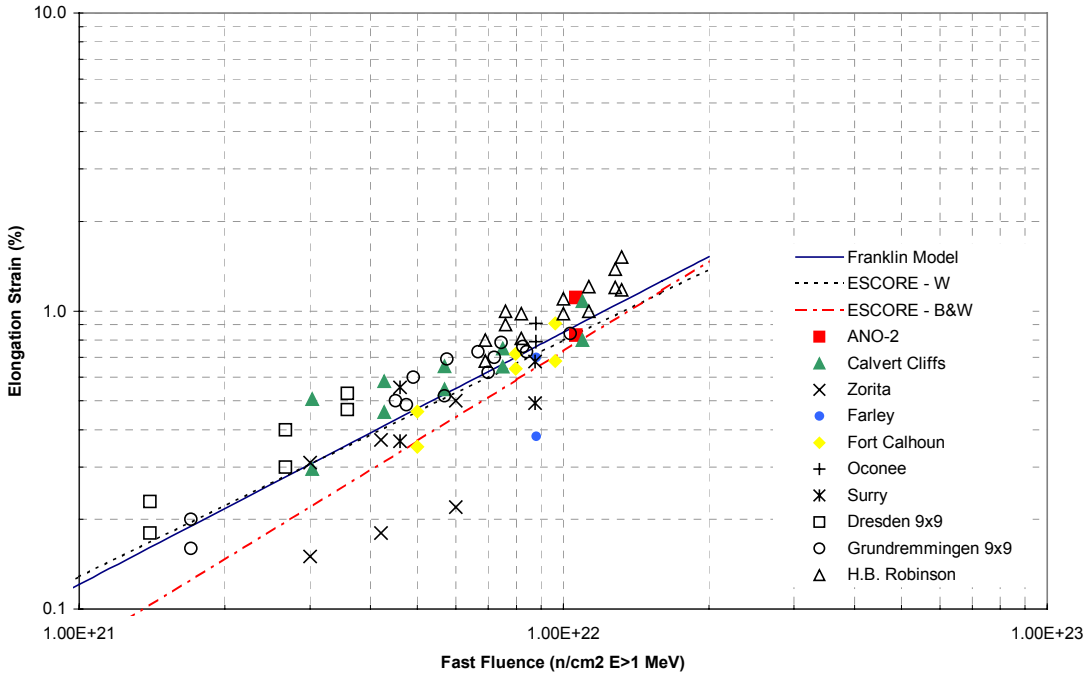

Figure 2-6
Comparison of the Irradiation Growth Models in FALCON with Post-Irradiation Examination Results for CWSR Zirconium Alloys

Both the ESCORE and Franklin Zr-4 irradiation growth models included in the FALCON Beta release version of the code will be tested using additional fuel rod length measurement data available in the FALCON V&V database.

Analysis Capabilities

FALCON contains appropriate models for the steady state analyses required to define transient initial conditions or for fuel diagnostic evaluations. These models include fission gas release, burnup, fuel cracking and relocation, local gap thickness and conductance, cladding and fuel viscoplasticity, fuel hot-pressing, swelling and densification, and pellet-cladding interaction (PCI). Because of the versatility of FALCON's finite element structure, these calculations can be carried out for full-length rods, short segments, or slices. The geometric models in these analyses consist of R-Z or R-θ grids as appropriate, the latter being more suited for PCI analysis. FALCON's PCI analysis capabilities are unique in that they permit the detailed simulation in the R-θ plane of discrete pellet cracks and pellet-cladding interfacial forces.

The following is a list of parameters, computed by FALCON, which are generally needed for licensing and fuel performance evaluation:

- Fuel Stored Energy
- Fuel Centerline Temperature
- Fuel Temperature Distribution
- Departure from Nucleate Boiling and Critical Heat Flux
- Cladding Inner and Outer Surface Temperatures
- Gap Thickness and Conductance Distributions
- Void Volume
- Fission Gas Release Fraction and Composition
- Gas Pressure
- PCI Damage Index
- Oxide Thickness
- Cladding Stress Distribution
- Cladding Strain Distribution
- Axial Growth

Operational transients, which are characterized by small changes in plant variables, and non-LOCA accidents, which include infrequent and limiting fault events, constitute the primary analysis targets for FALCON and thus are well within the range of validity of the material and physical models employed in FALCON. The licensing limits for operational transients are the SAFDLs (Specified Acceptable Fuel Design Limits) that are calculated and output by FALCON. The licensing limits for non-LOCA accidents are fuel enthalpy, peak cladding temperature, and

cladding oxidation. Fuel enthalpy and peak cladding temperature are inherent to the analysis and are printed in the output. Two cladding oxidation models are available to predict high temperature cladding oxidation. The thermal hydraulic model in FALCON allows operation of the code without the need for interfacing with system or transient thermal hydraulic programs for problems where closed-channel thermal hydraulics calculations are valid.

The following is a list of parameters calculated by FALCON that are currently needed to evaluate the fuel licensing limits.

- Thermal:
  - Heat Flux
  - Critical Heat Flux Ratio
  - Fuel Enthalpy
  - Fuel Centerline Temperature
  - Cladding Temperatures
- Mechanical:
  - Fission Gas Release
  - Internal Rod Pressure
  - Fuel-Cladding Contact Pressure
  - Cladding Stress
  - Cladding Strain
- Chemical:
  - Cladding Oxidation
  - Cladding Wall Thinning

Transients involving large-break LOCAs are the most limiting applications of FALCON. The program's capabilities in this area are limited to the heatup portion of the LOCA. However, FALCON contains extensive interface capabilities through user input of power, heat transfer coefficients, and bulk temperatures as functions of time and axial position, which permit the analysis of a wide range of such transients. A large number of axial nodes (up to 75 axial nodes in the fuel stack) can be used, permitting accurate treatment of the strong axial coupling associated with the reflood-quench portion of the LOCA. Also, the R-θ modeling capability of FALCON makes it possible to analyze the effects of azimuthal variations in temperatures on cladding ballooning and rupture.

As part of the peer review, a comparison of FALCON with several other fuel modeling codes was conducted. This comparison is periodically updated as part of the model development process. This ensures that key fuel behaviors are included in FALCON’s development activities and provides a current metric illustrating FALCON’s capabilities as compared to other available programs. Table 2-7 presents the comparison matrix of fuel modeling characteristics and capabilities for FALCON and other modeling codes. The table lists characteristics pertaining to

fuel rod representation, general code analysis applications, fuel pellet behavior, fuel-cladding gap and cladding behavior, coolant heat transfer and miscellaneous capabilities such as refabricated rod representation, barrier fuel, burnable absorbers and MOX. The comparison shown in Table 2-7 highlights the advanced modeling capabilities of FALCON compared to similar fuel behavior codes. The ENIGMA code, with all its behavioral models, is the only code of similar caliber to FALCON [38]. However, this code is limited primarily to operational transients and has little application to postulated accidents such as RIA and LOCA. The most noticeable deficiency in the FALCON code is the lack of a gaseous swelling model. Addition of this model will be completed in a later version of the code.

Recent Applications

Although still under development, FALCON has proven itself to be a useful computational tool for numerous problems pertinent to the industry. Recent applications include the review of new BWR fuel rod designs for utilities, RIA experimental analysis, analytical support for the Argonne National Laboratory (ANL) / NRC LOCA experimental program, and support for the revision of NRC criteria for the dry storage of high burnup (> 45 GWd/MTU) spent nuclear fuel [41, 2,42,43].

In the case of the RIA, LOCA, and spent fuel analyses, special purpose/developmental versions of FALCON have been developed to address these specific technical areas. Typically this involves development of fuel, cladding, coolant, and/or other phenomenological models to accommodate a particular behavior not previously available in the code. Brief descriptions of the special purpose versions of the code are shown below.

- FALCON Beta RIA
  Specific models added and/or modified include: burnup dependent fuel melting, critical strain energy density (CSED), fuel radial power profile, and fuel-cladding bonding.
- FALCON LOCA
  Specific models added and/or modified include: high temperature cladding oxidation, cladding surface temperature boundary condition specification (axial distribution, time-dependent).
- FALCON Spent Fuel
  Specific models added and/or modified include: post irradiation cladding creep. This version was developed to test creep models applicable to spent fuel storage conditions. Although complete, this version is experimental and is not finalized.

Another aspect to the special purpose FALCON versions is that they provide a test bed for model and code development. These versions leverage the FALCON development program by providing an opportunity to develop and test models that might not otherwise be added to the code in a rigorous development and application environment with funding from other programs. Typically the code changes required for these versions, often including additional code input and output options, are incorporated into the standard developmental version of FALCON. The primary model changes from the three special purpose FALCON versions noted above will be included in the upcoming Beta release of FALCON in 2003.

Table 2-7
Code Comparison Matrix

	FALCON	ESCORE	FREY	FRAPCON	ENIGMA	SCANAIR [39]	SIERRA [40]
Fuel Rod Representation							
1D Stacked Slices	X	X		X	X	X	X
2D R-Z	X		X				
Local Effects/Defects	X		X				
Applications							
Steady State	X	X		X	X		X
Transient	X		X		X	X	X
Fuel Pellet Behavior							
Grain Growth	X	X			X		X
Densification	X	X	X	X	X		X
Solid Swelling	X	X	X	X	X		X
Gaseous Swelling		X			X	X	X
Creep/Hot Pressing	X		X		X		?
Plasticity	X		X		X	X	X
Relocation	X	X	X	X	X		X
Cracking	X	X	X		X	X	X
Steady State Xe/Kr Rel.	X	X	X	X	X		X
Transient Xe/Kr Rel.	X		X		X	X	X
I-131 Release					X		
Pellet Hourglassing	X		X		X		X
Fuel Clad Gap Behavior							
Gas/Solid Conductance	X	X	X	X	X	X	X
PCMI	X	X	X	X	X	X	X
Stick/Sliding Interaction	X		X			X	
Pellet-Clad Bonding	X				X		
Axial Gas Mixing					X		
Cladding Behavior							
Irr. and Thermal Creep	X	X	X	X	X		X
Irradiation Growth	X	X		X	X		X
Irradiation Hardening	X		X	X	X	X	X
Plastic Deformation	X		X	X	X	X	X
Ballooning/Rupture	X		X				
PCI/ISCC	X		X		X		
Low Temp. Oxidation	X	X		X	X		X
High Temp. Oxidation	X		X				
Coolant Heat Transfer							
Steady State Flow	X	X	X	X	X	X	X
Transient Flow	X		X			X	
Post-CHF Heat Transfer	X		X			X	
Miscellaneous							
Include Refabrication					X		
Barrier Fuel	X		X				?
MOX	X				X	X	?
Burnable Absorbers	X	X	X	X	X		?

References

1. "FALCON – Fuel Analysis and Licensing Code, Vol. 1: Summary Report on Development Activities," ANATECH Report ANA-97-0230, December 1997.

2. Montgomery, R.O., Rashid, Y.R., "FALCON BETA-RIA: Fuel Analysis for Reactivity Initiated Accident, Vol. 1: Theoretical and Numerical Bases," ANATECH Report ANA-02-0356, October 2002.

3. Moore, K. V., et al., "RETRAN - A Program for One-Dimensional Transient Thermal-Hydraulic Analysis of Complex Fluid Flow Systems," Volume 1, EPRI CCM-5, December 1978.

4. Stewart, C. W., "VIPRE-01: A Thermal-Hydraulic Code for Reactor Cores, Volume 1: Mathematical Modeling (Revision 2)," NP-2511-CCM, July 1985.

5. "MATPRO - Version 11: A Handbook of Materials Properties for Use in the Analysis of Light Water Reactor Fuel Rod Behavior," NUREG/CR-0497 TREE-1280, February 1979.

6. Lyon, W.F. et al., "Fuel Cladding Mechanical Property Data Assessment and Evaluation," Final Report, TR-1003134, EPRI, Palo Alto, CA, September 2001.

7. Gilmore, P.M., Klepfer, H.H., Sorensen, J.M., "EPRI PWR Fuel Cladding Corrosion (PFCC) Model, Volume 1: Theory and User's Manual," TR-105387-V1, EPRI, Palo Alto, CA December 1995.

8. Ross, A.M., Stoute, R.L., "Heat Transfer Coefficient between $U0_2$ and Zircaloy-2," CRFD-1075, Chalk River, Ontario, June 1962.

9. Todreas, N., Jacobs, G., "Thermal Conductance of Reactor Fuel Elements," *Nuclear Science and Engineering*, 50, 1973, p. 283.

10. Rashid, Y.R., Montgomery, R.O., Zangari, A.J., "FREY-01: Fuel Rod Evaluation System, Vol. 1: Theoretical and Numerical Bases," Revision 3, Final Report, EPRI NP-3277, EPRI, Palo Alto, CA, August 1994.

11. Gates, G.A., White, R.J., "Start-of-Life Gap Conductance Measurements on SBR Mixed Oxide Fuel," *Proceedings of the ANS International Topical Meeting on LWR Fuel Performance*, Park City, Utah, April 10-13, 2000, pp. 696-705.

12. Freeburn, H. R., Ozer, O., Yang, R., "The Effect of Burnup on UO_2 Thermal Conductivity - NRC Review of the ESCORE Model," *Enlarged Halden Programme Group Meeting on Fuels and Materials Performance and Computerized Man-Machine Communication*, Bolkesjo, Norway, June 9-14, 1991.

13. Lippens, M., Mertens, L., "High Burnup UO_2 and (U,Gd)O_2 Specimens: Thermal Diffusivity Measurements and Post-Irradiation Characterization," Final Report, TR-106501, X102-22, EPRI, Palo Alto, CA, 1996.

14. Turnbull, J. A., "An Empirical Model Describing the Degradation of UO_2 Thermal Conductivity with Burn-Up Based on Laser Flash Measurements of Thermal Diffusivity," TR-111347, EPRI, Palo Alto, CA, 1998.

15. Amaya, M., et al., "Thermal Conductivities of Irradiated UO_2 and (U,Gd)O_2 Pellets," *IAEA Technical Committee Meeting on Nuclear Fuel Behaviour Modelling at High Burnup and Its Experimental Support*, Windermere, UK, June 18-23, 2000.

16. Fukushima, S., et al., "The Effect of Gadolinium Content on the Thermal Conductivity of Near-Stoichiometric (U,Gd)O_2 Solid Solutions," *Journal of Nuclear Materials 105*, 1982, pp. 201-210.

17. Newman, L. W., et al., "Thermal and Physical Properties of Urania-Gadolinia Fuel," DOE/ET/34212-43, Department of Energy, May 1984.

18. Watson, R. H., "Properties of the Urania-Gadolinia System (Part 2)," Final Report, NP-5861-LD, EPRI, Palo Alto, CA, 1988.

19. Turner, S.E., et al., "Background and Derivation of ANS-5.4 Standard Fission Product Release Model," NUREG/CR-2507, January 1982.

20. Ritterbusch, S.E., et al., "Factors Affecting Post-DNB Operation for Light Water Reactors, Volume 1," EPRI NP-1999, RP 1382-1, August 1981.

21. Kramman, M.A., Freeburn, H. R., Eds., "ESCORE--the EPRI Steady-State Core Reload Evaluator Code: General Description," EPRI NP-5100, EPRI, Palo Alto, CA, February 1987.

22. Forsberg, K., Massih, A.R., "Diffusion Theory of Fission Gas Migration in Irradiated Nuclear Fuel UO_2," *Journal of Nuclear Materials 135*, 1985, pp.140-148.

23. Turnbull, J.A., Private Communication, March 2002.

24. Bernard, L.C., Jacoud, J.L., Vesco, P., "An Effcicient Model for the Analysis of Fission Gas Release," *Journal of Nuclear Materials 302*, 2002, pp. 125-134.

25. Hagrman, D.T., "SCDAP/RELAP5/MOD 3.1 Code Manual, MATPRO – A Library of Materials Properties for Light Water Reactor Accident Analysis," NUREG/CR-6150, June 1995.

26. Limbäck, M., Andersson, T., "A Model for Analysis of the Effect of Final Annealing on the In- and Out-of-Reactor Creep Behavior of Zircaloy Cladding," *Zirconium in the Nuclear Industry: Eleventh International Symposium, ASTM STP 1295*, American Society for Testing and Materials, 1996, pp. 448-468.

27. Franklin, D.G., "Zircaloy-4 Cladding Deformation During Power Reactor Irradiation," *Zirconium in the Nuclear Industry: Fifth Conference*, ASTM STP 754, American Society for Testing and Materials, 1982, pp. 235-267.

28. Gorscak, D. A., Pfenningworth, P.L., "Analysis of Cladding Deformation over Plenum Axial Gaps in Zircaloy Clad Fuel Rods," WAPD-TM-1339, December 1982.

29. Hobson, D.O. et. al., "Effects of Temperature and Pressure on te In-Reactor Creepdown of Zircaloy Fuel Cladding," *Zirconium in the Nuclear Industry: Fifth Conference*, ASTM STP 754, American Society for Testing and Materials, 1982, pp. 173-192.

30. Matsuo, Y., "Thermal Creep of Zircaloy-4 Cladding Under Internal Pressure," *Journal of Nuclear Science and Technology 24 [2],* 1987, pp. 111-119.

31. Hoppe, N.E., "Engineering Model for Zircaloy Creep and Growth," *Proceedings of ANS-ENS International Topical Meeting on LWR Fuel Performance*, Avignon, France, April 21-24, 1991, pp. 201-209.

32. Papazoglou, T.P., Davis, H.H., "EPRI/B&W Cooperative Program on PWR Fuel Rod Performance," Final Report, NP-2848, EPRI, Palo Alto, CA, March 1983.

33. Gilbon, D. et al., "Irradiation Creep and Growth Behavior, and Microstructural Evolution of Advanced Zr-Based Alloys," *Zirconium in the Nuclear Industry: Twelfth International Symposium, ASTM STP 1354*, American Society for Testing and Materials, 2000, pp. 51-73.

34. McGrath, M.A., "In-Reactor Creep Behaviour of Zircaloy Cladding," *Proceedings of the ANS International Topical Meeting on LWR Fuel Performance*, Park City, Utah, April 10-13, 2000, pp. 137-150.

35. Matsuo, Y., "Creep Behavior of Zircaloy under Variable Conditions," *Zirconium in the Nuclear Industry: Eighth International Symposium, ASTM STP 1023*, American Society for Testing and Materials, 1989, pp. 678-691.

36. Bouffioux, P., Rupa, N., "Impact of Hydrogen on Plasticity and Creep of Unirradiated Zircaloy-4 Cladding Tubes," *Zirconium in the Nuclear Industry: Twelfth International Symposium, ASTM STP 1354*, American Society for Testing and Materials, 2000, pp. 399-422.

37. Berna, G.A., et al., "FRAPCON-3: A Computer Code for the Calculation of Steady-State, Thermal-Mechanical Behavior of Oxide Fuel Rods for High Burnup," NUREG/CR-6534, December 1997.

38. Palmer, I., Rossiter, G., White, R., "Development and Validation of the ENIGMA Code for MOX Fuel Performance Modelling," IAEA-SM-358/20, IAEA MOX Fuels Symposium, Vienna, May, 1990.

39. Lamare, L., Latche, J.C., "SCANAIR A Computer Code for Reactivity Initiated Accidents in LWRs," Rapport Technique Semar 95/01, Service D'Etudes Et De Modelisation D'Accidents De Reacteurs, IPSN, Cadarache, France, Sept. 1995.

40. Billaux, M.R., et al., "SIERRA: A Fuel Performance Code to Predict the Mechanical Behavior of Fuel Rods to High Burnup," *Proceedings of the International Topical Meeting on LWR Fuel Performance*, Portland, Oregon, March 2-6, 1997.

41. Sunderland, D., "Assessment of GE14 Cladding Hoop Stress and Pre-Conditioning Linear Power Threshold for the Brunswick Nuclear Plant," ANATECH Report ANA-02-0354, October 2002.

42. "Test Plan for the Investigation of High-Burnup LWR Cladding Under LOCA and Other Transient Conditions," IPS-263-Rev. 1, Argonne National Laboratory, October 1997.

43. Rashid, Y.R., Dunham, R.S., "Creep Modeling and Analysis Methodology for Spent Fuel in Dry Storage," Final Report, TR-1003135, EPRI, Palo Alto, CA, November 2001.

3
SOLUTION PROCEDURE AND THEORY

This section presents a brief discussion of the solution technique used in FALCON. A detailed derivation of the theory and implementation including the governing equations and the physical and material models employed is available in the theory document recently published for the FALCON Beta RIA version [1]. Some changes have been implemented in the code since the development of the Beta RIA version. These changes, as they pertain to the solution technique, will be highlighted. The following sections will address the implementation of the finite element method spatial model, heat transfer and deformation computations, and the numerical procedure including steady state and transient coupling.

Spatial Model

Three types of finite element spatial models are employed to define the fuel rod geometry depending upon the type of simulation desired. The first two, Mode 1 and Mode 2, are used to represent an R-Z plane axial cross section of a fuel rod assuming symmetry along the rod centerline. The Mode 1 grid is a one-dimensional (1D) axial segment stacking approach similar to that used in ESCORE. This model features axially decoupled, 1D radial elements with three nodes and three integration (Gauss) points. This mode was implemented in order to allow FALCON to more closely duplicate the computational technique employed in ESCORE. The Mode 2 grid is a 2D, R-Z plane model that is fully axially and radially coupled featuring nine node and nine Gauss point quadrilateral elements in the fuel and cladding. Figure 3-1 is an illustration of Mode 1 and Mode 2 spatial models. Also shown is a comparison of the 1D and 2D elements used in each.

The Mode 3 spatial model is a fully radially and azimuthally coupled 2D, R-θ model of a cross sectional slice across a fuel rod. As with the Mode 2 model, the Mode 3 model also uses nine node and nine Gauss point quadrilateral elements in the fuel and cladding. As mentioned in earlier sections of this report, this model represents a unique computational capability in FALCON. The Mode 3 model is used primarily for PCI and local effects analyses and can simulate discrete pellet cracks and pellet-cladding interfacial forces. Figure 3-2 is an illustration of a typical Mode 3 spatial model.

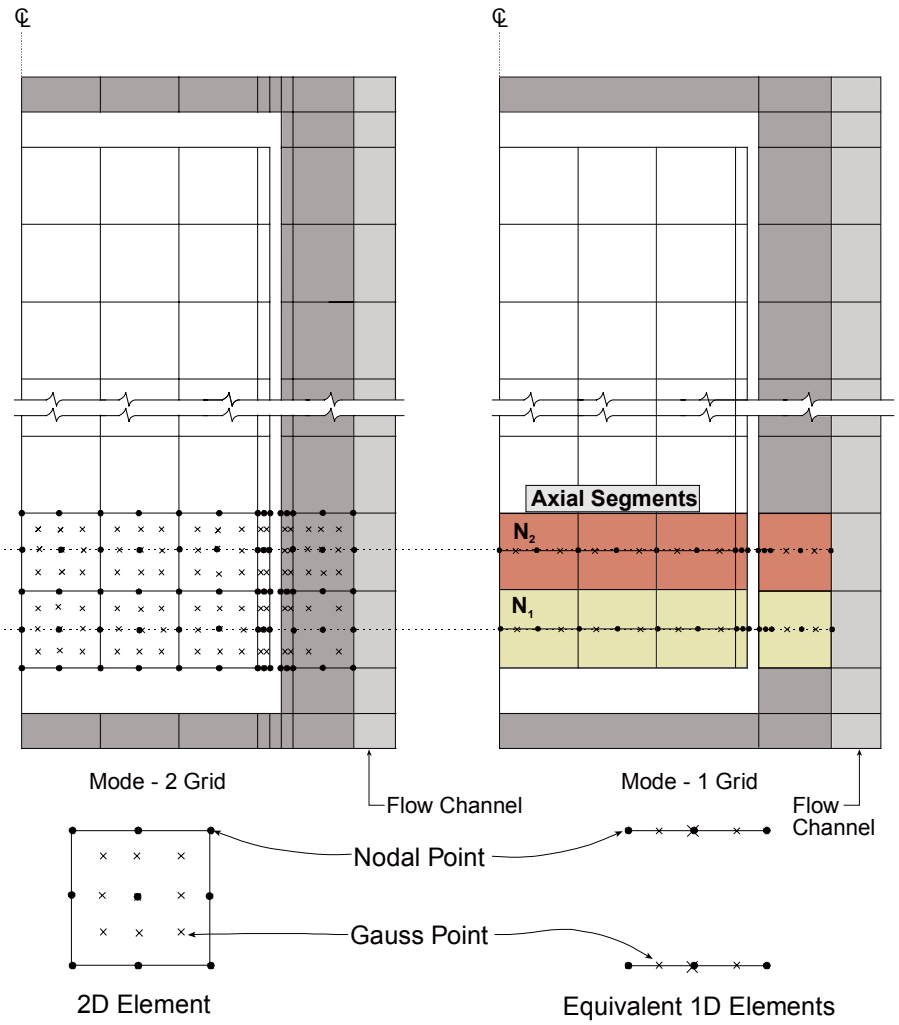

Figure 3-1
Mode 1 and Mode 2 Finite Element R-Z Plane Spatial Models

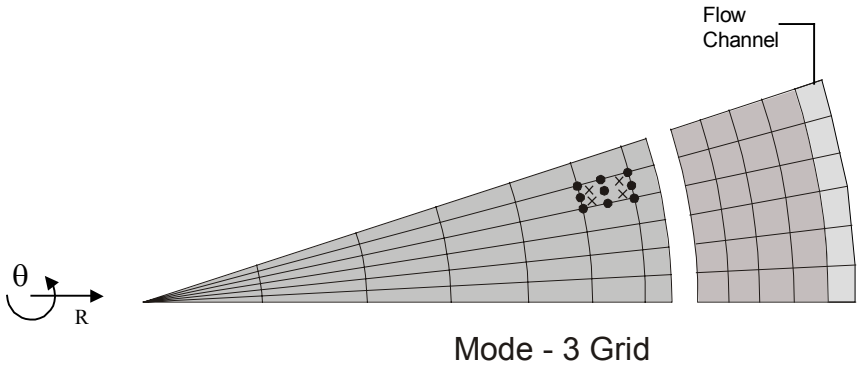

Figure 3-2
Mode 3 Finite Element R-θ Plane Spatial Model

Heat Transfer

Under normal operating conditions, heat transfer in a fuel rod is generally governed by five primary mechanisms: (1) heat generation in the fuel, (2) conduction through the fuel pellets, (3) combined conduction and radiative heat transfer across the pellet-cladding gap, (4) conduction though the cladding and cladding oxide layer, and (5) convective heat transfer to the coolant. In FALCON, the heat generation sources are fission, gamma heating, decay of fission products, and the heat of oxidation (zirconium-oxygen reaction on the cladding surface). The material properties governing conduction through the fuel rod, the fuel and cladding conductivities, specific heats and densities, are generally temperature and burnup dependent. The gap conductance is computed using fuel and cladding conductivity (for closed gaps), fuel and cladding surface roughness, interfacial pressure between fuel and cladding, Meyer-Hardness of the cladding, gas thermal conductivity using the modified Ross and Stoute model for an open gap, and Mikic-Todreas model as modified by Lanning and Hann in BNWL-1894 for a closed gap [2,3,4]. Convective heat transfer from the fuel rod surface is based on the coolant temperature and the heat transfer coefficient. The latter can be either user-specified or calculated using the flow channel model.

In FALCON, the transient heat conduction equations are formulated in terms of the finite element spatial model. Temperatures are calculated at the nodal points within each element (see Figure 3-1) from the boundary and thermal conditions specified. The spatial model formulation for each problem, i.e. the sizes, shapes and types of the elements, is defined based on the accuracy requirements and the physical and material characteristics of each region. For example, the fuel and the cladding are represented by nine-node elements in which the spatial variation of temperature is a quadratic function. Whereas the gap is represented by two-node elements with linear temperature variation since the heat transfer in this region is governed primarily by the gap conductance. As an example of the size of a typical R-Z spatial model, the Full-5 library model contains a total of 123 elements and 313 nodes. The governing equations of the overall system are formulated with the nodal temperatures as the primary unknowns. This system is piece-wise linear in time and is solved implicitly with provisions for iteration within each step and/or sub-division of the time steps into smaller sub steps.

The volumetric heat generation rate is calculated at several spatial positions (Gauss points – see Figure 3-1) in the fuel, cladding, and coolant elements using the rod average linear power, axial power profile and radial power distribution. The axial power profile is time-dependent and is treated by FALCON as user input. The radial power profile can either be defined by user input or calculated using one of two available radial power distribution models, RADAR-G and TUBRNP [5,6]. A fraction of the energy produced by fission in the fuel is deposited in the cladding and the coolant by gamma radiation. A heat generation term for gamma heating in the cladding and the coolant, expressed as a percentage of the total fuel rod power, is available as a user input parameter. The heat generation due to the radioactive decay of fission products is calculated in FALCON using the methods described in the 1979 ANS-5.1 Standard [7]. The fission-product decay heat is determined for the thermal fission of ^{235}U and ^{239}Pu and fast fission of ^{238}U as a function of time following shutdown and prior reactor operating conditions. Decay heat from other actinide or activation products or neutron capture by the fission products is not considered. It is assumed that the axial power shape for decay heat production follows the axial power shape prior to reactor shutdown. The radial power profile is assumed to be uniform. This approach provides an approximate power spatial variation within the fuel rod for use in

FALCON. Heat generation due to cladding corrosion (conversion of zirconium to ZrO_2) is calculated using a model from MATPRO.

The other major components inside the fuel rod affecting heat transport are the plenum regions, the upper plenum being of primary importance. In FALCON, the upper plenum is modeled essentially as a large gap. It is defined using elements assigned the appropriate thermal and mechanical properties representing the spring material and stored gases. The plenum conductance is computed using the spring (if present) and gas conductivities and the spring radiative heat transfer coefficient using the same methodology as an open fuel-cladding gap ignoring the temperature jump distances.

The thermal boundary conditions for the fuel and cladding temperature calculations can be determined using the coolant enthalpy model, or through user specification of either the heat transfer coefficient and coolant (bulk) temperature distribution, the wall heat fluxes, or the cladding surface temperatures. This gives FALCON the ability to model a large variety of thermal conditions and greatly enhances the functionality of the code. The coolant channel is subdivided into control volumes, each of which coincides to a cladding element. The input inlet conditions for the mass flow rate, fluid temperature or enthalpy, and pressure are used to initialize the model at the lower plenum. For each control volume, the inlet conditions at the lower interface are used to solve for the exit conditions at the upper interface.

The coolant enthalpy model also has the ability to treat both water and sodium coolants. For water, FALCON models both single-phase (liquid or vapor) and two-phase fluid flow and heat transfer. A complete representation of the forced convection boiling curve for water is included. For sodium, the coolant enthalpy rise model only considers single-phase (liquid) fluid flow and convective heat transfer. As noted previously, the heat transfer and critical heat flux correlations in FALCON are based on those used in the RETRAN and VIPRE codes [8,9]. A detailed description of the coolant enthalpy rise model including discussions of the heat transfer, critical heat flux correlations, and the water and sodium properties used in FALCON is presented in the FALCON Beta RIA theory manual [1].

The user should note that the coolant channel model is based on a homogeneous closed channel approach, with thermal equilibrium between the liquid and vapor phases. This approach simplifies the required computations; however, no consideration is given to pressure losses or lateral momentum, or energy transfer to adjacent channels. In addition, pressure and flow feedback is not modeled (i.e., no flow oscillations). These effects may be of importance for fuel rod bundle flow and the user should take the limitations of this approach into consideration. The coolant channel model in FALCON is adequate for scoping calculations and for single rod/single channel experiments similar to those used to benchmark the program. For these conditions, selection of the appropriate heat transfer and critical heat flux correlations that comply with the conditions to be analyzed will provide the user with reasonable results.

Deformation

The system of equations that characterize the deformation of the fuel rod is comprised of: (1) the strain-displacement relations, (2) the stress-strain constitutive relations, (3) the boundary conditions, and (4) the equilibrium equations. The strain-displacement relations that govern the kinematic behavior of the fuel rod are of critical importance to the modeling of the large deformation ballooning behavior of the cladding. For application in FALCON, finite-strain theory is utilized for the cladding and infinitesimal strain theory is applied to the fuel where the deformations are expected to remain small.

The use of finite deformation theory for the cladding permits FALCON to model ballooning (or collapse) under differential pressure. This state of large deformation evolves in a continuous manner in the solution, thus avoiding an artificial switch to a "ballooning model". However, in the fuel, deformation remains in the domain of the infinitesimal strain theory; therefore, the strain-displacement relations for the fuel elements do not require the nonlinear terms. The material behavior represented covers the entire range from initial elastic response to the elastic-plastic-creep, strain-rate-sensitive response in the high power and temperature regimes. The equilibrium equations are derived in incremental form based on the principle of virtual work subject to the appropriate boundary conditions and consist of piecewise linear algebraic equations that compute the nodal displacements using the nodal forces. This system of equations is solved implicitly using an iterative time-stepping procedure. For further details on the derivation of these equations and their application in FALCON, the reader is referred to the FALCON Beta RIA theory manual [1].

Numerical Procedures

The governing equations for the heat transfer portion of the problem are formulated as a system of equations relating the heat flow vector to the nodal temperatures of the current and previous time step using the Galerkin error minimization method and the Crank-Nicholson central differencing technique. The deformation portion of the problem is formulated using the virtual work variational principle and a forward differencing algorithm with a Newton iteration technique. The resulting system of equations relates the nodal forces to the nodal displacement increments at each time step. Principles of continuum thermomechanics are rigorously applied in both formulations, thus maintaining theoretically consistent and continuous behavior for the fuel rod as it undergoes various thermal and deformation regimes from low temperature, small deformation response, to high temperature, large deformation response.

Using time-dependent input and previous step information (or initial condition information for the first time step), the thermal solution is computed first, and the nodal temperatures are calculated using an efficient frontal solver. The incremental displacements are then obtained, using as input the nodal temperatures, the internal and external pressure distributions, and the specified boundary constraints. The same frontal solver is used in the deformation solution except for that the computations involve a vector field as opposed to the scalar field used in the thermal solution. The element strains and stresses are calculated at designated Gauss points within the fuel, cladding, and gap elements. Updated feedback variables, such as gap size

distribution, fuel-cladding contact conditions, gas pressure, etc., are accounted for in the iteration solution.

Recent changes in the iteration procedure have been implemented to address gap convergence/chattering problems noted under certain conditions during steady state testing. For rods with low gap conductance due to either large initial gap widths or predominately Xe-filled gaps, numerical oscillations in both gap size and gap conductance, and therefore temperature, were noted. The iteration procedure was modified to improve the convergence of the thermal and mechanical solutions. Figure 3-3 illustrates the computed gap thickness for IFA 562.1 Rod 10, a Xe-filled rod.

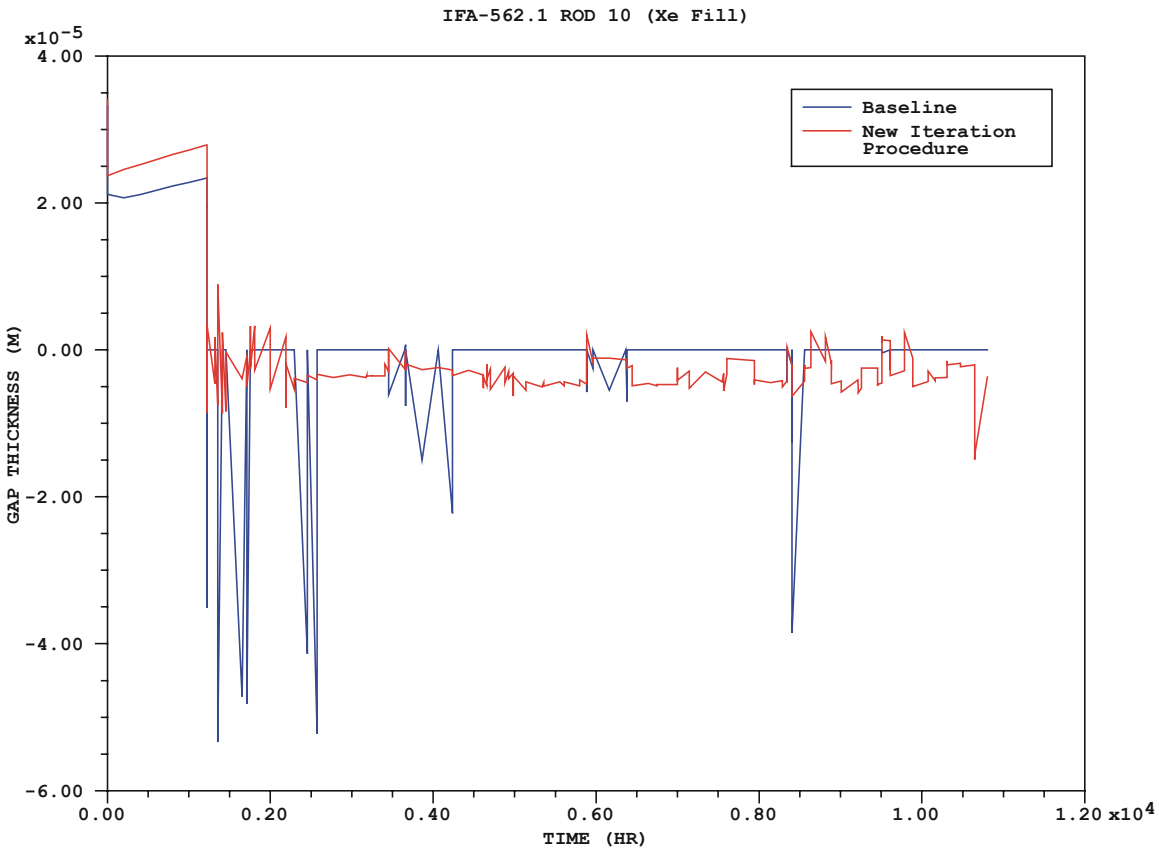

Figure 3-3
Comparison of Computed Gap Thickness as a Function of Irradiation Time for IFA 562.1 Rod 10 (Xe-Filled rod)

The plot shows that the new iteration procedure eliminates the large oscillations characteristic in the gap thickness computed previously (referred to as the baseline). This improvement appears to have solved the numerical oscillation problem, but further fine tuning of the iteration procedure will likely occur as benchmarking activities continue.

The iteration procedure executed during each time step is comprised of three primary iteration loops: one each for the thermal and mechanical solutions, and a third outer iteration loop that encompasses both solutions. Figure 3-4 is a diagram of the revised iteration procedure where NTHERM, NMECH, and NITER refer to the number of thermal, mechanical, and overall

solution iterations, respectively. At a time, t, the time step is initiated by conducting a thermal analysis using the current conditions for the coolant and power. The mechanical results from the previous time step, t - Δt, are used to establish the gap conditions required in the gap conductance calculation. The thermal solution loop iterates six times for steady state conditions. For transient conditions, a sub stepping procedure is also used that computes thermal conditions at additional times limited by the change in power. Next, the mechanical analysis is conducted using the latest thermal results produced to define the temperature dependent material properties, and the thermal forces and expansion strains. The mechanical solution loop iterates four times and produces a new deformation state that changes the fuel-cladding gap status, and thus the gap conductance. This procedure is then repeated in the outer iteration loop. The number of outer iterations is currently available as an input option. The recommended number of outer iterations is five. Additional refinement of the iteration procedure is anticipated as benchmarking and testing activities continue. Ultimately, both thermal and mechanical convergence criteria will be implemented that control the iterative procedure.

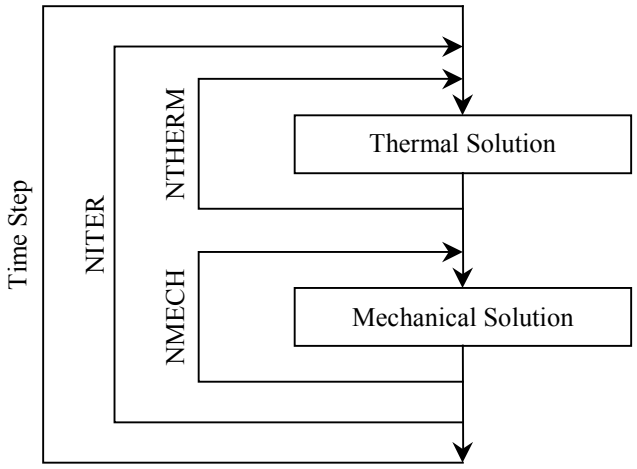

Figure 3-4
Diagram of Revised Iteration Procedure

Steady State to Transient Coupling

As noted previously, one of the primary goals of the development of FALCON is to eliminate the need to couple steady state and transient analyses produced by two different computer codes. This has been achieved by incorporating the 1D solution methodology along with specific steady state analysis modules used by ESCORE into FALCON. By design, the 1D and 2D grids used in FALCON are compatible making the transition between one to the other seamless and transparent to the user. Temperatures and displacements, computed at element nodes are directly transferred at common nodal positions and interpolated at non-common nodal positions. Similarly, state variables computed at element Gauss points, are transferred at common Gauss points and extrapolated at non-common Gauss points. A zero-time iteration is then performed for equilibration. This provides the user the capability run steady state and transient analyses in series, switching between 1D and 2D grids and timescales as needed. Steady state analyses can be also run in the full 2D mode, which eliminates the need for any data translation, internal or otherwise.

Although complete steady state analyses can be developed using FALCON's input format, FALCON retains the capability to run ESCORE input decks directly. In this case, the analysis defaults to the 1D mode. Alternatively, FALCON can translate an ESCORE input deck into a FALCON input deck. This alternative allows the user to utilize an existing steady state analysis as the basis for a one in FALCON. Once in FALCON's input format, the steady state analysis can be run in a stand-alone mode, or coupled with a transient analysis as required.

References

1. Montgomery, R.O., Rashid, Y.R., "FALCON BETA-RIA: Fuel Analysis for Reactivity Initiated Accident, Vol. 1: Theoretical and Numerical Bases," ANATECH Report ANA-02-0356, October 2002.

2. Ross, A.M., Stoute, R.L., "Heat Transfer Coefficient between UO_2 and Zircaloy-2," CRFD-1075, Chalk River, Ontario, June 1962.

3. Todreas, N., Jacobs, G., "Thermal Conductance of Reactor Fuel Elements," *Nuclear Science and Engineering*, 50, 1973, p. 283.

4. Lanning, D.D., Hann, C.R., "Review of Methods Applicable to the Calculation of Gap Conductance in Zircaloy Clad UO_2 Fuel Rods," Battelle Pacific Northwest Laboratories, BNWL-1894, April 1975.

5. Thomas, G.M., Hesketh, K.W., "RADAR-G - A Routine for Calculating Radial Power Profiles in Thermal Reactor Fuel," BNFL, EPRI Contract 18362, November 1986.

6. Lassmann, K., O'Carroll, C., van de Loor, J., Walker, C. T., "The Radial Distribution of Plutonium in High Burnup UO_2 Fuel," *Journal of Nuclear Materials, 208*, 1994, pp. 2232-231.

7. "American National Standard for Decay Heat Power in Light Water Reactors," ANSI/ANS-5.1, 1979.

8. Moore, K. V., et al., "RETRAN - A Program for One-Dimensional Transient Thermal-Hydraulic Analysis of Complex Fluid Flow Systems," Volume 1, EPRI CCM-5, December 1978.

9. Stewart, C. W., "VIPRE-01: A Thermal-Hydraulic Code for Reactor Cores, Volume 1: Mathematical Modeling (Revision 2)," NP-2511-CCM, July 1985.

4
BENCHMARKING, VERIFICATION, AND VALIDATION

This section provides an overview of FALCON benchmarking and verification and validation (V&V) activities. The initial portion of this section will review the benchmarking and V&V approach which was presented in detail in the Alpha release document [1]. That document defined the strategy for the development of the fuel rod case database including the case selection criteria and prioritization. This section will also address the current status of benchmarking and V&V activities along with the presentation of selected results from code testing and development.

Approach

The initial task of the V&V plan was to develop an extensive database of analysis cases built upon the existing ESCORE and FREY V&V databases. The combination of these two databases has been supplemented with data from experiments and irradiation programs available since the completion of ESCORE and FREY. The priority for selection of these cases is an emphasis on data to support steady state analysis of extended duty and high burnup fuel. Since the fundamental basis of FALCON is the FREY code, transient benchmarking is not emphasized for the Beta release. It is assumed that the verification of the transient capability of the code is encompassed by the FREY and FALCON Beta RIA V&V activities. Additionally, recommendations from the review of the ESCORE V&V by S. M. Stoller were utilized [2,3,4]. In this review, criteria were established to provide guidance for future fuel performance code benchmarking. These criteria have been used to aid in the selection of cases for the steady state portion of the FALCON V&V database. The general characteristics of the supplementary cases selected to populate the database are summarized below.

- High burnup, grater then 50 GWd/MTU, up to or exceeding 70 GWd/MTU
- Representative of current fuel designs
- Representative of specific phenomena observed in high burnup fuel behavior, i.e. rim formation

Additional recommendations for fuel rod test cases were made during the peer review process. These focused primarily on instrumented research rods to be used for the development of specific fuel performance models within FALCON. For example, recommendations were made for cases to benchmark and/or verify fuel densification, relocation, fission gas release, thermal conductivity (including Gd-bearing fuel), and cladding creep. These recommendations were incorporated into the V&V database development plan.

Database Status

As noted in the Alpha release document, the population of fuel rod cases is generally divided into three groups: (1) instrumented research rods, (2) non-instrumented research rods, and (3) commercial fuel rods. The FALCON V&V plan designates rods from groups 1 and 2 to be used in benchmarking activities (model development, testing, and calibration) and those from group 3 for validation to demonstrate the code's predictive capability for commercial fuel rods. A small number of commercial rods from group 3 may also be used for benchmarking in instances where data from instrumented and non-instrumented research rods do not adequately represent, for example, high burnup fuel behavioral phenomena.

To date, over 680 cases representing a wide range of fuel design variants, irradiation environments, and burnups have been identified for potential inclusion into the FALCON V&V database. The sources for these cases include the ESCORE and FREY V&V databases, Halden test reactor programs (both from reports and from the Halden Test Fuel Database [TFDB]), and EPRI, U.S. Department of Energy, NRC, and commercial utility fuel test programs. Currently, 257 FALCON input decks have been developed and entered into the FALCON V&V database. The distribution of these is as follows: 163 instrumented and non-instrumented research rods, and 94 commercial fuel rods. These rods represent both PWR and BWR fuel types and burnups up to ~ 70 GWd/MTU. As of this writing additional cases are being prepared. These include an additional 21 instrumented research rods. Additionally, data has also been obtained for the preparation of an additional 127 commercial fuel rods. A listing of current cases comprising the FALCON V&V database along with source and development status information is attached in Appendix A. In addition, data sets that are currently being compiled are noted.

An analysis data request form was developed to facilitate gathering data for inclusion into the FALCON V&V database. This form lists detailed data requirements including fuel and cladding dimensions, thermal hydraulic parameters, rod design data, and power history/axial shape data needed for FALCON fuel performance analyses. Units and default values (if applicable) for the various parameters are also listed and prioritized. In addition, recommendations are included to specify the format of electronic data for power histories, axial shapes, and other distribution data such as that required for PWR corrosion analyses. The form is attached in Appendix B.

A subset of the FALCON V&V database has been designated for thermal benchmarking. This group of 17 cases was chosen specifically to evaluate gap conductance and FALCON's fuel rod thermal performance in the absence of significant fission gas release. The primary parameters affecting these cases were the initial diametral gap thickness, fill gas composition, and fuel surface roughness. This set of cases was also instrumental in diagnosing the gap convergence/chatter behavior in FALCON and in testing the changes implemented in the iterative solution procedure that eliminated this problem. Table 4-1 is a list of the thermal benchmarking tests cases and summary information describing the function of each experiment and the relevant fuel performance parameters.

Table 4-1
Thermal Benchmarking Cases

Test	**Description**
IFA 504	Gas Flow Experiment, Thermal Effects on Fuel 200 μm gap 10% enrichment 3 rods - He, Ar, Xe fill gases, evaluated during startup
IFA 505.5	Gap Size and Fill Gas Effect on Gap Conductance ~ 40 GWd/MTU burnup Rod 1: 10% enrichment, He-filled, 100 μm gap Rod 2: 6% enrichment, Xe-filled, 100 μm gap Rod 3: 10% enrichment, Xe-filled, 50 μm gap
IFA 509.1	Gap Size Effect on Gap Conductance ~ 14 GWd/MTU burnup All rods 10% enrichment, He-filled Rod 1: 150 μm gap Rod 2: 225 μm gap Rod 3: 60 μm gap
IFA 515.10	Thermal Behavior of Gd-Bearing Fuel ~ 50 –55 GWd/MTU burnup Both rods He-filled, 50 μm gap Rod A1: UO_2, 11.5% enrichment Rod A2: 8% Gd_2O_3, 13% enrichment
IFA 562.1	Effect of Surface Roughness and Fill Gas on Gap Conductance ~ 14 GWd/MTU burnup All rods 3.95% enrichment, 60 – 72 μm gap Rod 5: He-filled, 0.78 μm fuel roughness Rod 6: He-filled, 1.38 μm fuel roughness Rod 7: Xe-filled, 0.55 μm fuel roughness Rod 10: Xe-filled, 1.5 μm fuel roughness Rod 11: He-filled, 0.45 μm fuel roughness Rod 12: He-filled, 1.3 μm fuel roughness

Thermal Benchmarking

Several iterations have been performed using the thermal benchmarking cases. As noted above, these cases were chosen to evaluate the effects of fundamental fuel rod characteristics such as fill gas, gap size, surface roughness, etc., on the thermal performance of FALCON. Several sensitivity studies were conducted during the thermal benchmarking iterations by varying numerous models and parameters to assess their effect on the computed results. These included evaluations of the fuel radial power profile model, fuel densification models, and the method of thermal boundary condition designation. The aforementioned gap convergence/chattering problem was tied to rods with low gap conductance (do to either large initial gap widths or predominately Xe-filled gaps). The effect was particularly acute for large initial gap rods with Xe fill gas due to enhanced thermal feedback under these conditions. It was also noted that, in general, temperature calculations for Xe-filled rods consistently over predicted the measured values. Evaluation of this effect led to the improvements in the FALCON iterative solution

technique noted in Section 3. Selected results from the thermal benchmark test cases listed in Table 4-1 are presented below.

The first set of plots, Figures 4-1 through 4-5, illustrate the analysis of He-filled rods by comparing FALCON computed centerline temperatures to the measured values. Unlike the plots in Figures 4-2 through 4-5, the data for IFA 504 presented in Figure 4-1 represents the initial startup ramp and plots fuel temperature as a function of linear power. Due to cycling in the power history (see insert Figure 4-1) and effects such as fuel cracking and relocation, the plotted FALCON results cycle within a narrow band for a given linear power.

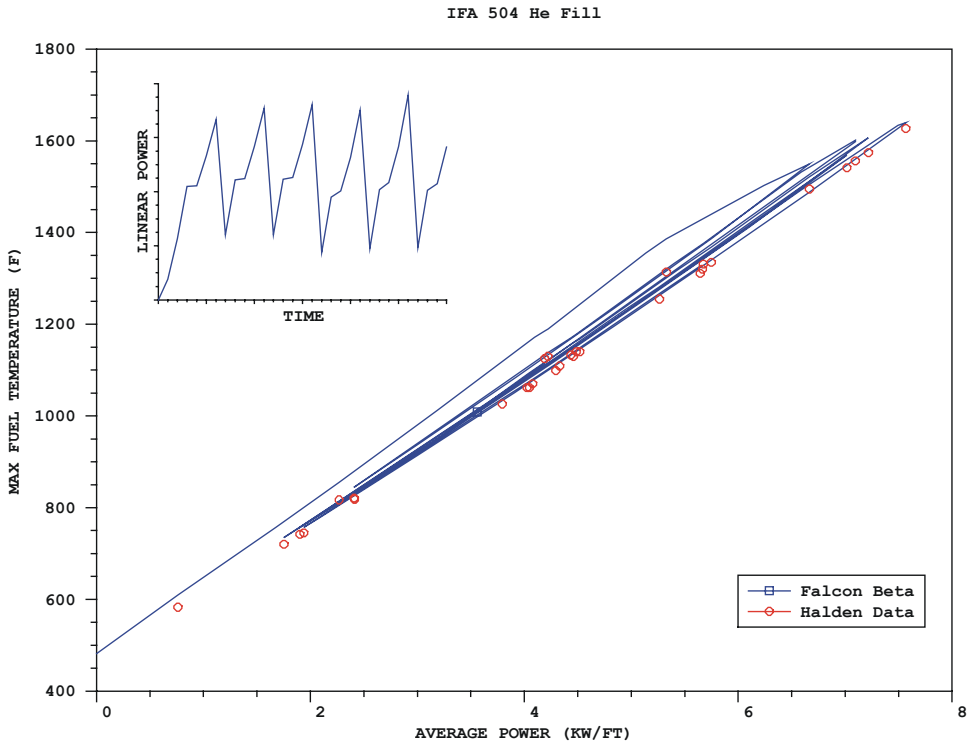

Figure 4-1
Maximum Fuel Centerline Temperature as a Function of Linear Power for IFA 504 (He-Filled Rod)

To provide a uniform basis of comparison, a statistical analysis program was developed to compare FALCON computations to the experimental measurements. This program computes the difference between the measured value and the temperature computed by FALCON at each point in the measured temperature time history and compares that difference to the average temperature experienced during the test to compute a standard deviation. Based on the analysis of the temperature results from the He-filled rod cases, FALCON achieves an overall standard deviation of ± 4.75%. Figures 4-6 through 4-8, illustrate FALCON computed centerline temperatures for Xe-filled rods. As with Figure 4-1, the data plotted in Figure 4-6 represents power cycle data from the initial ramp for IFA 504. Due to the presence of Xe and the resulting thermal feedback effects, the results indicate larger cycling in the fuel temperatures.

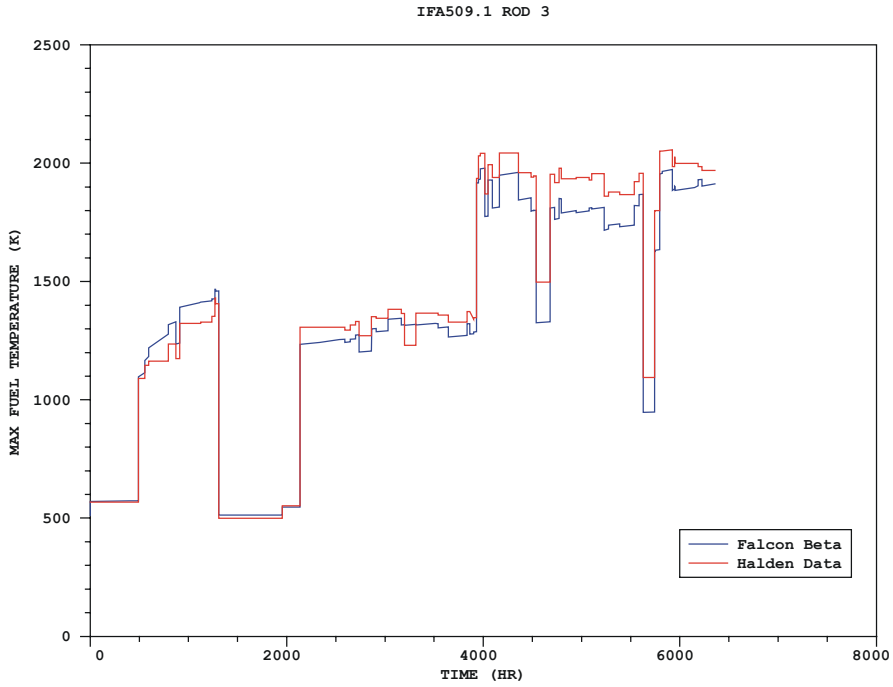

Figure 4-2
Maximum Fuel Centerline Temperature as a Function of Irradiation Time for IFA 509.1, Rod 3 (He-Filled Rod)

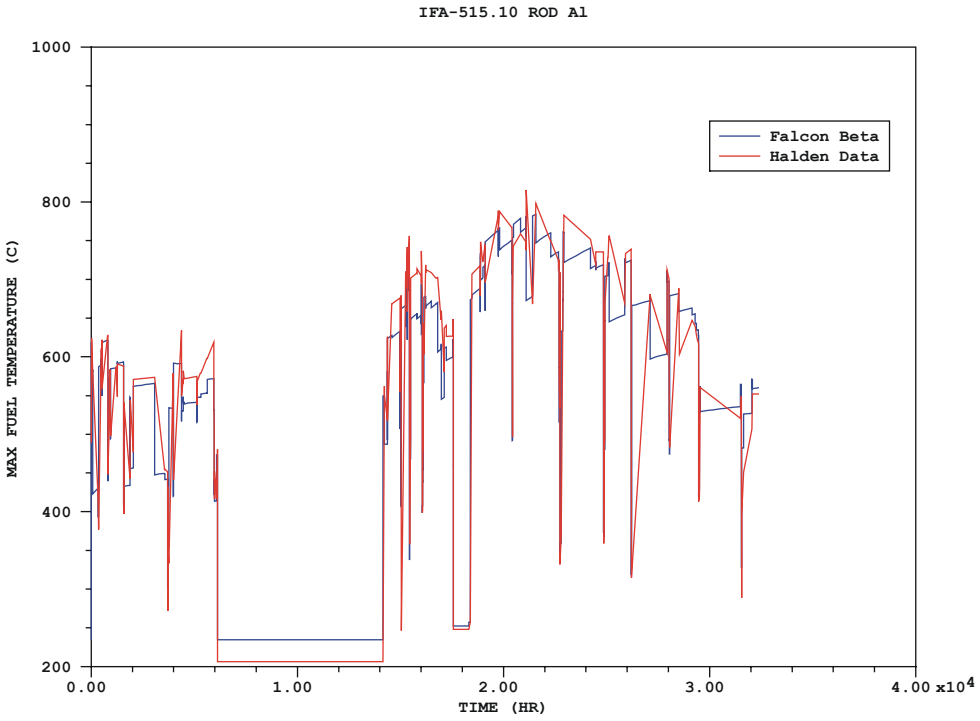

Figure 4-3
Maximum Fuel Centerline Temperature as a Function of Irradiation Time for IFA 515.10, Rod A1 (He-Filled Rod)

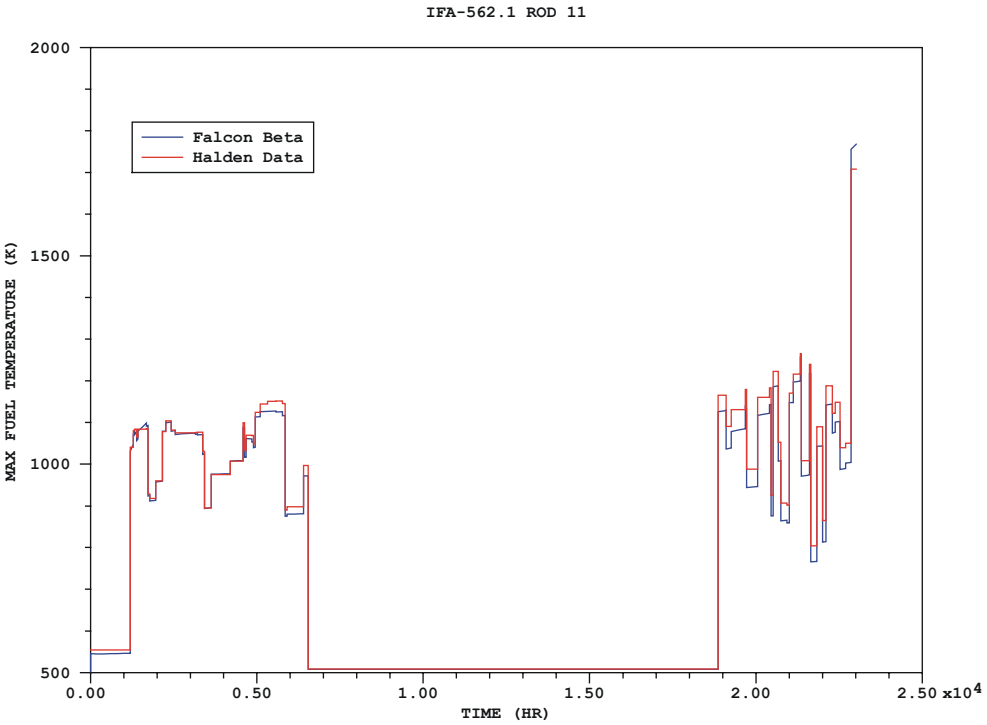

Figure 4-4
Maximum Fuel Centerline Temperature as a Function of Irradiation Time for IFA 562.1, Rod 11 (He-Filled Rod)

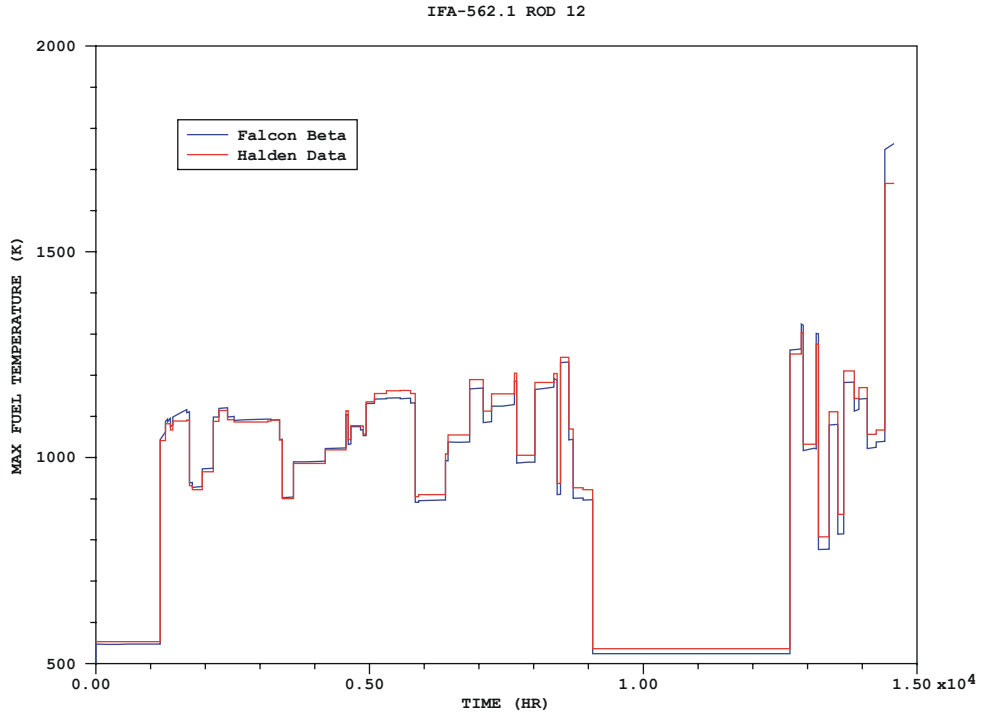

Figure 4-5
Maximum Fuel Centerline Temperature as a Function of Irradiation Time for IFA 562.1, Rod 12 (He-Filled Rod)

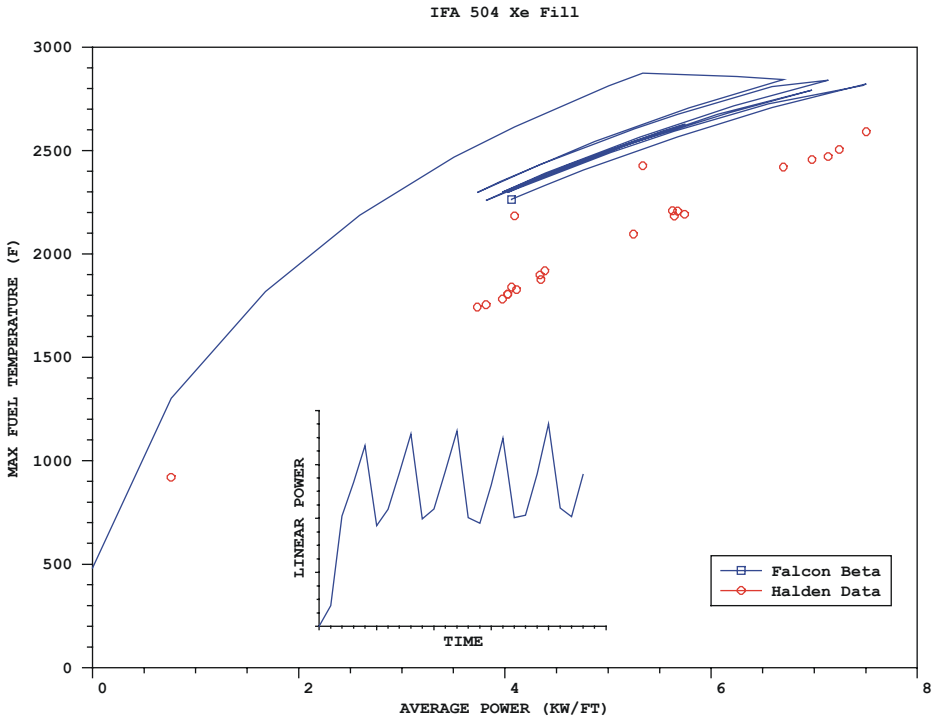

Figure 4-6
Maximum Fuel Centerline Temperature as a Function of Linear Power for IFA 504 (Xe-Filled Rod)

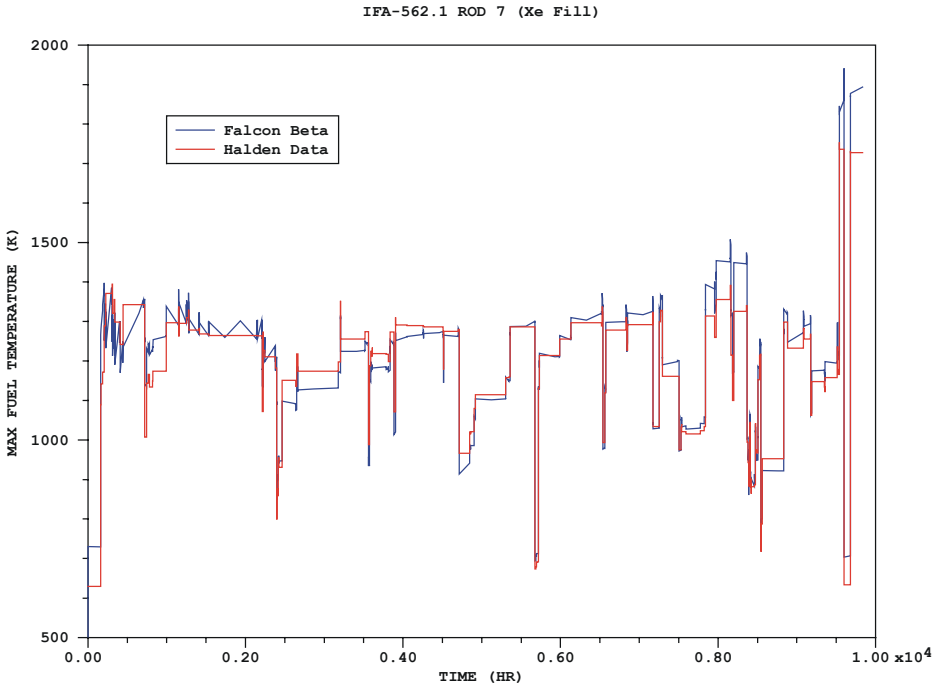

Figure 4-7
Maximum Fuel Centerline Temperature as a Function of Irradiation Time for IFA 562.1, Rod 7 (Xe-Filled Rod)

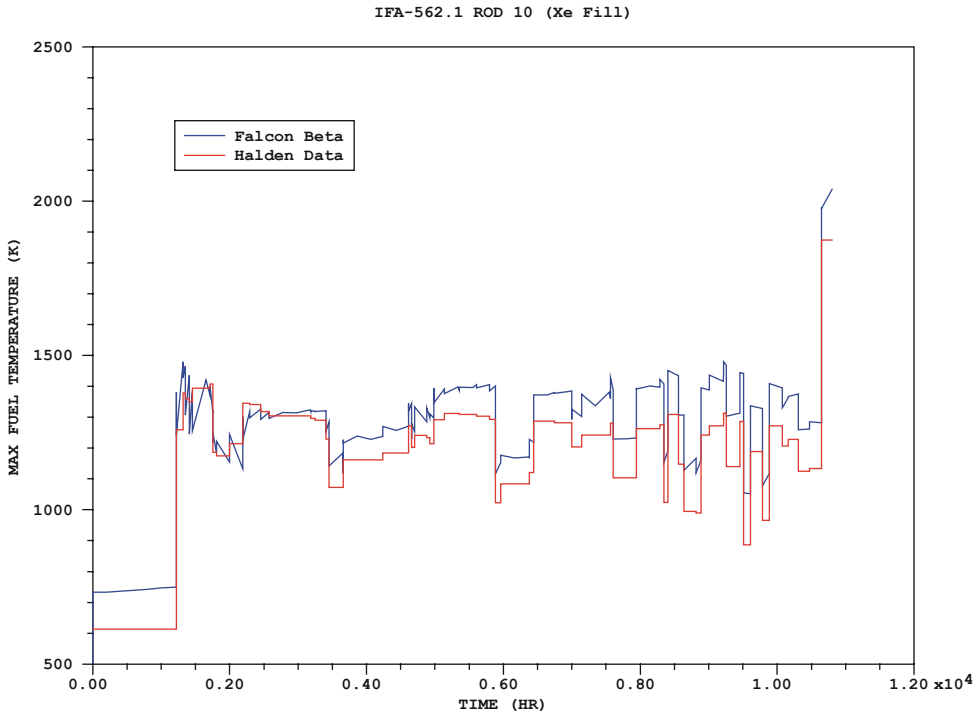

Figure 4-8
Maximum Fuel Centerline Temperature as a Function of Irradiation Time for IFA 562.1, Rod 10 (Xe-Filled Rod)

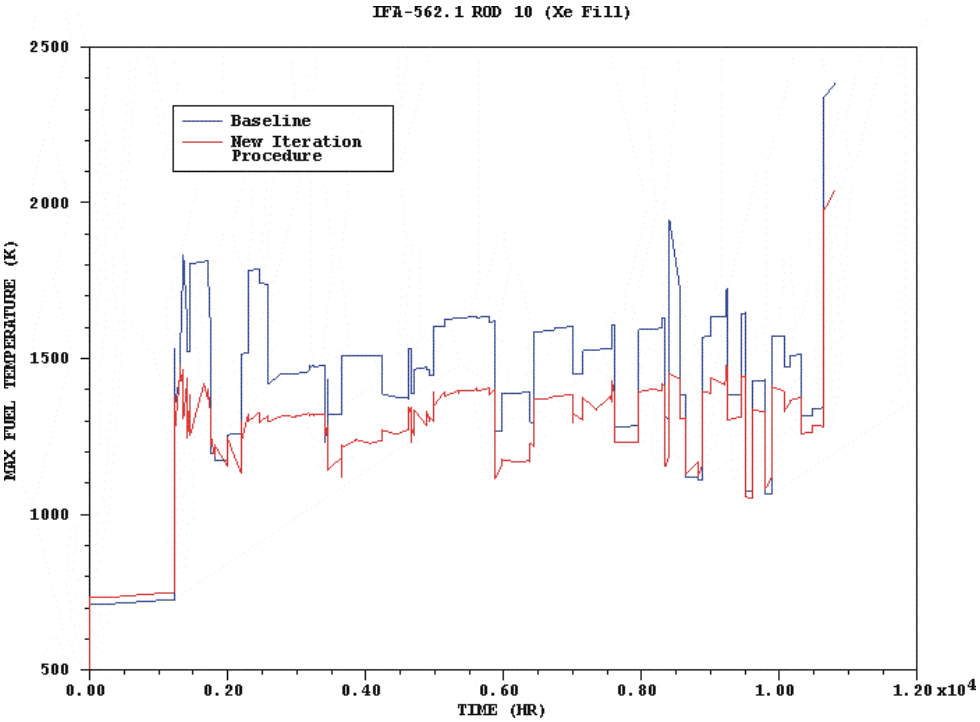

Figure 4-9
Comparison of Maximum Fuel Centerline Temperature as a Function of Irradiation Time for Different Iteration Procedures for IFA 562.1, Rod 10 (Xe-Filled Rod)

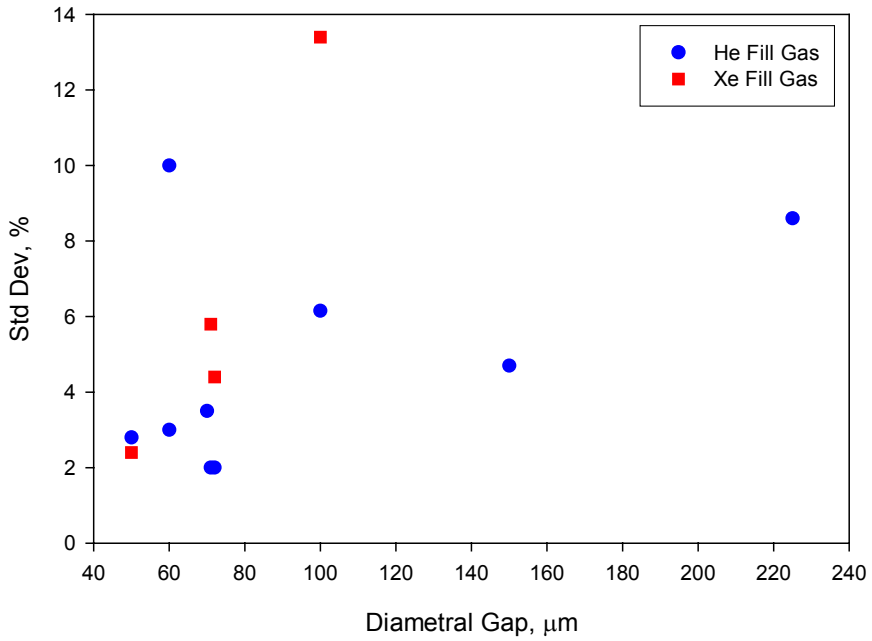

Figure 4-10
Standard Deviation of Maximum Fuel Centerline Temperature as a Function of Initial Diametral Gap for He- and Xe-Filled Rods

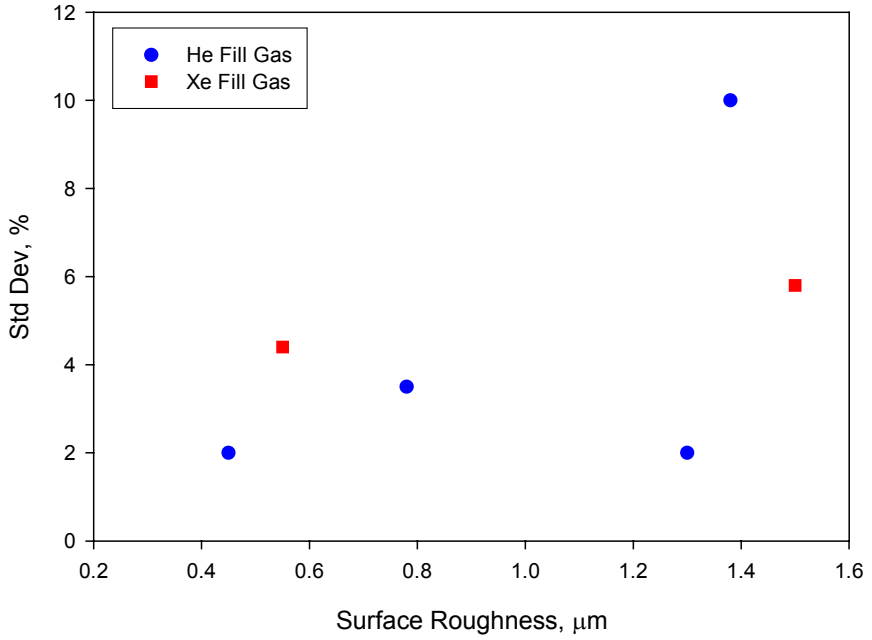

Figure 4-11
Standard Deviation of Maximum Fuel Centerline Temperature as a Function of Fuel Surface Roughness for He- and Xe-Filled Rods

Evaluation of the results from the Xe-filled rod analyses indicates that FALCON tends to over predict the temperatures for these rods at higher burnups. As a result, the overall standard deviation of the FALCON temperature calculations for Xe-filled rods is somewhat higher than that for the He-filled rods at ± 6.5%. Figure 4-9 plots the FALCON computed centerline temperatures comparing the results from the old (baseline) and the new iteration procedures using data from IFA 562.1 Rod 10. This plot indicates a large decrease in the predicted temperature using the new iteration procedure bringing the predicted value to within a standard deviation of ± 5.8%, an improvement over previously obtained results.

Figures 4-10 and 4-11 were developed to evaluate the overall trends in the temperature calculations as functions of initial gap thickness and fuel surface roughness. Figure 4-10 shows a discernable trend of increasing standard deviation with initial diametral gap thickness indicating a potential bias in the gap conductance computation. The data plotted in Figure 4-11 is limited to rods from IFA 562.1, an experiment designed specifically to evaluate fuel surface roughness effects. Figure 4-11 appears to indicate a trend of increasing standard deviation with fuel surface roughness although not nearly as strong as with initial diametral gap thickness.

A summary of the results for temperature analysis of the thermal benchmark cases is provided in Table 4-2. Overall, the results of the thermal benchmarking tests and sensitivity studies indicate marked improved in the steady state thermal performance of FALCON from previous versions. This has been achieved through a combination of improvements in the iterative solution technique as well as refinement in the modeling options used for these rods. Further improvement is anticipated as benchmarking and calibration activities continue.

Table 4-2
Thermal Benchmarking Cases Results Summary[1]

TestCase	Fuel Centerline Temperature Standard Deviation	
	°C	%
IFA 505.5		
Rod 1	71	6.15
Rod 2	177	13.4
Rod 3	28	2.4
IFA 509.1		
Rod 1	68	4.7
Rod 2	135	8.6
Rod 3	48	3
IFA 515.10		
Rod A1	16.7	2.8
Rod A2	73	11
IFA 562.1		
Rod 5	36	3.5
Rod 6	103	10
Rod 7	51	4.4
Rod 10	71	5.8
Rod 11	22	2
Rod 12	22	2

1 – IFA 504 test cases are not included due to limitations in the statistical analysis program.

References

1. "FALCON – Fuel Analysis and Licensing Code, Vol. 1: Summary Report on Development Activities," ANATECH Report ANA-97-0230, December 1997.

2. Sunderland, D., Harbottle, J., "An Assessment of the Validation of the ESCORE I Code," Stoller Report to S. Levy for EPRI Project 2061-26, August 1991.

3. Sunderland, D., Harbottle, J., "Selection of Rods to Re-Evaluate ESCORE I by Use of Discriminating Criteria," Stoller Report to S. Levy for EPRI Project 2061-26, August 1991.

4. Sunderland, D., Harbottle, J., "Review of New Fuel Performance Data," Stoller Report to S. Levy for EPRI Project 2061-26, August 1991.

5
SUMMARY AND FUTURE ACTIVITIES

FALCON is a combined steady state and transient fuel behavior code developed for the analysis of a single fuel rod under normal operation, operational transients, postulated accidents, and post irradiation spent fuel behavior under storage conditions. The development of FALCON represents the state-of-the-art in LWR fuel performance modeling. The numerical structure of the program is based on the finite element methodology, which provides a robust and versatile code framework to test and incorporate improved thermal and mechanical material property models and pellet and cladding behavioral subprograms. Furthermore, the finite element methods utilized in FALCON allow for flexible geometric representation of the fuel rod, including stacked one-dimensional axial slices, as well as, full two-dimensional fuel rod and local effects models. The fuel rod model in FALCON is coupled to a single channel coolant enthalpy rise model that contains a full representation of the single and two-phase boiling heat transfer curve for water. FALCON can also model single-phase liquid heat transfer conditions for flowing sodium.

FALCON is a combination of the transient fuel behavior analysis capabilities from FREY and the steady state fuel performance capabilities from ESCORE. Both of these codes in the past have proven to be useful in the analysis of fuel rod performance for either normal operation or postulated accident applications. However, using ESCORE to initialize the transient analysis in FREY was difficult and added a level of complexity and uncertainty in the transient analysis of high burnup fuel. The combination of steady state and transient analysis capabilities in FALCON provides a seamless transition from the steady state analysis required to initialize fuel rod conditions at the start of a transient to the transient fuel behavior analysis used to evaluate high burnup response during operational transients and postulated accidents. FALCON can transition between the steady state and transient modes of analysis multiple times during a problem. Such an intimate coupling of the steady state and transient capabilities allows the analysis of high burnup fuel under accident conditions without a cumbersome initialization procedure and the added uncertainty of model and computational differences.

FALCON Development Summary

The development activities for the Beta release version of FALCON have focused on the pellet and cladding material and behavior models required for steady state fuel performance analysis, with an emphasis to upgrade these models for high burnup applications, where appropriate. The areas of development include:

- Cladding irradiation and thermal creep, irradiation growth, and both low temperature and high temperature outer surface oxidation
- Pellet relocation, densification, melting, and thermal conductivity

- Radial power and burnup distribution
- Steady state fission gas release
- Pellet rim formation
- Fission gas release enhancement in the pellet rim

In addition to the modifications and improvements in the material and behavioral models in FALCON, Beta version development has incorporated improvements in the numerical structure of the program. A more robust numerical iteration scheme has been implemented to enhance the convergence behavior of the temperature and displacement solutions. Also, the coupled thermal and mechanical iteration convergence on the pellet cladding gap conductance was improved. The new iteration techniques will improve the behavior of the program for analyses of xenon filled rods and fuel rods susceptible to thermal feedback mechanisms leading to large fission gas release.

An important element in the FALCON BETA version development is the code benchmarking and validation activities. Because of the complex thermal, mechanical, and chemical behavior of a fuel rod, a fuel rod modeling code requires benchmarking to ensure that the coupling of the different empirical and mechanistic behavioral models produces satisfactory results. A database of irradiated fuel rods has been developed from which fuel rod cases will be selected to include in the FALCON benchmarking and validation. More than 680 fuel rods have been identified for potential inclusion in the irradiated fuel rod database. These rods represent a wide range of fuel rod designs, irradiation conditions, burnup levels, and in-pile and post-irradiation examination results. From this database, more than 250 FALCON input decks have been developed for use in the benchmarking and validation process. These rods include both instrumented test reactor rods and commercial reactor fuel rods. The selected rods represent both PWR and BWR fuel designs and burnup levels up to 70 GWD/MTU.

In parallel to the development and benchmarking activities, FALCON has been used in support of recent industry needs. These applications include:

- Fuel rod design evaluations
- Analysis of RIA tests and development of revised RIA acceptance criteria
- Analytical support of the ANL-NRC LOCA program
- Support of dry storage of high burnup spent fuel

The results of the FALCON calculations have proved useful in support of these industry applications.

Future Development Activities

The FALCON Beta release version represents an interim code release that will be used to test the program capabilities and identify coding errors. An important element of the Beta release is to obtain user feedback regarding the functionality of FALCON for fuel performance analysis needs. The future development activities include verification and validation of FALCON for

steady state and transient analyses up to rod average burnup levels above 70 GWd/MTU, improvement of user input and output capabilities, and incorporation of code improvements based on user feedback. FALCON continues to be used to support industry efforts related to RIA, LOCA, and spent fuel storage. As they become available from these efforts, specific models related to transient fission gas release and gaseous swelling under RIA conditions, high temperature cladding deformation during a LOCA event, and thermal creep under dry storage conditions will be incorporated into future versions of FALCON. The initial Beta release version of FALCON will be available for testing at the end of 2002. Its primary focus will be the analysis capabilities for steady state behavior, including centerline temperature, fission gas release, cladding creep down, and fuel rod axial growth. Benchmarking and V&V activities will continue into the first quarter of 2003 followed by the final release of the Beta version along with the relevant code documentation in the second quarter of 2003.

Lastly, the FALCON peer review process has and will continue to provide important guidance and suggestions on model improvements and expanded verification and validation. The authors would like to acknowledge the contributions of the reviewers C. Bernaudat, J.A. Turnbull, and D.R. Olander. Many of the recommendations from the peer review process have been incorporated through model development and testing activities. Others that are still under consideration will be evaluated and incorporated into FALCON as needed to maintain a fuel performance code that contains the latest knowledge of fuel behavior at high burnup.

A
APPENDIX A

The following pages contain tables listing the rods in the FALCON V&V database. The tables are organized into two primary sections, instrumented and non-instrumented research rods and commercial program rods and include comments on the source of the data for each case and its status. The data were taken from a variety of sources including reports and electronic data files provided by EdF (S. Beguin and J. Claudel, "Halden Input Deck for EPRI," E-N-T-CN/01-00569, 2001).

Two additional tables, also broken down into these two categories, list rods that are under development for inclusion into the database. The instrumented and non-instrumented research rods under preparation consist of IFA cases from the Halden Test Fuel Data Bank (TFDB) system. The commercial rods currently under preparation come from three irradiation programs. The first is from the PROTOTYPE Program conducted at Calvert Cliffs-1. These rods were irradiated in 14 x 14 assemblies for five cycles. The assemblies were discharged in 1988 with an assembly average burnup of 57.4 GWd/MTU and a peak rod burnup of 63.5 GWd/MTU. The second set of commercial rods was part of a lead assembly program conducted at the Grohnde PWR in Germany. Two 16 x 16 assemblies were irradiated for four cycles reaching average burnups of 46 GWd/MTU. The third group was a set of specially fabricated rods, comprising five cladding variants, irradiated for a maximum of four cycles in a test assembly in the Gösgen PWR in Switzerland. These rods reached burnups in the range of 41 to 51.4 GWd/MTU. Additional commercial rods under consideration for the FALCON V&V database include rods from the OSIRIS and GAIN programs available through the International Fuel Performance Experiments Database (IFPE) and rods from an EPRI-sponsored hot cell program related to failed fuel at the Leibstadt BWR (KKL) in Switzerland.

Table A-1
Instrumented and Non-Instrumented Research Rods

Case	Rod	Comment
IFA409.2	807	Rod 807 preliminary analysis completed. Under final review. Data from Halden project reports.
IFA409.2	808	Rod 807 preliminary analysis completed. Under final review. Data from Halden project reports.
IFA 432.1	1	Draft input deck completed. Converted from ESCORE V&V/Re-Eval deck.
IFA 432.2	2	Draft input deck completed. Converted from ESCORE V&V/Re-Eval deck.

Table A-1 (continued)
Instrumented and Non-Instrumented Research Rods

Case	Rod	Comment
IFA 432.3	3	Draft input deck completed. Converted from ESCORE V&V/Re-Eval deck. Measurement data also extracted from TFDB.
IFA 504	He	Initial analyses completed. Only ramp temperature data available. Hydraulic diameter data also evaluated (electronic data available from EdF files[1]).
IFA 504	Ar	Initial analyses completed. Only ramp temperature data available. Hydraulic diameter data also evaluated (electronic data available from EdF files[1]).
IFA 504	Xe	Initial analyses completed. Only ramp temperature data available. Hydraulic diameter data also evaluated (electronic data available from EdF files[1]).
IFA 505.5	1	Initial analyses completed, data from EdF files
IFA 505.5	2	Initial analyses completed, data from EdF files
IFA 505.5	3	Initial analyses completed, data from EdF files
IFA 509.1	1	Initial analyses completed, data from EdF files
IFA 509.1	2	Initial analyses completed, data from EdF files
IFA 509.1	3	Initial analyses completed, data from EdF files
IFA 515.10	A1	Initial analyses completed, data from EdF files
IFA 515.10	A2	Initial analyses completed, data from EdF files
IFA 533.2	807	Preliminary analysis completed. Data from Halden project reports.
IFA 533.2	808	Preliminary analysis completed. Data from Halden project reports.
IFA 534.14		Data extracted from TFDB. Decks to be developed.
IFA 558		Data extracted from TFDB. Decks to be developed.
IFA 562.1	5	Initial analyses completed, data from EdF files
IFA 562.1	6	Initial analyses completed, data from EdF files
IFA 562.1	7	Initial analyses completed, data from EdF files
IFA 562.1	10	Initial analyses completed, data from EdF files
IFA 562.1	11	Initial analyses completed, data from EdF files
IFA 562.1	12	Initial analyses completed, data from EdF files
IFA 597.2	2	Preliminary analysis completed. Data from Halden project reports.
IFA 597.3	3	Preliminary analysis completed. Data from Halden project reports.
IFA 629.2		Data extracted from TFDB. Decks to be developed.

Table A-1 (continued)
Instrumented and Non-Instrumented Research Rods

Case	Rod	Comment
IFA 636.1		Data extracted from TFDB. Decks to be developed.
RISO III	AN2	Initial analyses completed, data from ESCORE V&V/Re-Eval decks, data files, and project reports.
RISO III	AN3	Initial analyses completed, data from ESCORE V&V/Re-Eval decks, data files, and project reports.
RISO III	AN4	Initial analyses completed, data from ESCORE V&V/Re-Eval decks, data files, and project reports.
RISO III	GE4	Initial analyses completed, data from ESCORE V&V/Re-Eval decks, data files, and project reports.
RISO III	GE7	Initial analyses completed, data from ESCORE V&V/Re-Eval decks, data files, and project reports.
HBEP GE	10-1	Initial analyses completed, data from ESCORE V&V/Re-Eval decks, data files, and project reports.
HBEP GE	10-2	Initial analyses completed, data from ESCORE V&V/Re-Eval decks, data files, and project reports.
HBEP GE	14-2	Initial analyses completed, data from ESCORE V&V/Re-Eval decks, data files, and project reports.
HBEP W	17A	Initial analyses completed, data from ESCORE V&V/Re-Eval decks, data files, and project reports.
Tribulation W	109	Initial analyses completed, data from ESCORE V&V/Re-Eval decks, data files, and project reports.
Tribulation W	217	Initial analyses completed, data from ESCORE V&V/Re-Eval decks, data files, and project reports.
Tribulation W	220	Initial analyses completed, data from ESCORE V&V/Re-Eval decks, data files, and project reports.
Tribulation W	324	Initial analyses completed, data from ESCORE V&V/Re-Eval decks, data files, and project reports.
HBC BN	1066	Initial analyses completed, data from ESCORE V&V/Re-Eval decks, data files, and project reports.
HBEP ABB	8-4	Initial analyses completed, data from ESCORE V&V/Re-Eval decks, data files, and project reports.
HBEP ABB	8-6	Initial analyses completed, data from ESCORE V&V/Re-Eval decks, data files, and project reports.
HBEP ABB	6-4	Initial analyses completed, data from ESCORE V&V/Re-Eval decks, data files, and project reports.
HBEP ABB	27-6	Initial analyses completed, data from ESCORE V&V/Re-Eval decks, data files, and project reports.
HBEP ABB	36-4	Initial analyses completed, data from ESCORE V&V/Re-Eval decks, data files, and project reports.

Table A-1 (continued)
Instrumented and Non-Instrumented Research Rods

Case	Rod	Comment
HBEP ABB	36-6	Initial analyses completed, data from ESCORE V&V/Re-Eval decks, data files, and project reports.
HBEP BNFL	AK	Initial analyses completed, data from ESCORE V&V/Re-Eval decks, data files, and project reports.
HBEP BNFL	AL	Initial analyses completed, data from ESCORE V&V/Re-Eval decks, data files, and project reports.
HBEP BNFL	AP	Initial analyses completed, data from ESCORE V&V/Re-Eval decks, data files, and project reports.
HBEP BNFL	AU	Initial analyses completed, data from ESCORE V&V/Re-Eval decks, data files, and project reports.
HBEP BNFL	BH	Initial analyses completed, data from ESCORE V&V/Re-Eval decks, data files, and project reports.
HBEP BNFL	BK	Initial analyses completed, data from ESCORE V&V/Re-Eval decks, data files, and project reports.
HBEP BNFL	BN	Initial analyses completed, data from ESCORE V&V/Re-Eval decks, data files, and project reports.
HBEP BNFL	BP	Initial analyses completed, data from ESCORE V&V/Re-Eval decks, data files, and project reports.
HBEP BNFL	BW	Initial analyses completed, data from ESCORE V&V/Re-Eval decks, data files, and project reports.
HBEP BNFL	CQ	Initial analyses completed, data from ESCORE V&V/Re-Eval decks, data files, and project reports.
HBEP BNFL	DE	Initial analyses completed, data from ESCORE V&V/Re-Eval decks, data files, and project reports.
HBEP BNFL	DF	Initial analyses completed, data from ESCORE V&V/Re-Eval decks, data files, and project reports.
RISO	M20-1B	Initial analyses completed, data from ESCORE V&V/Re-Eval decks, data files, and project reports.
RISO	PA29-4	Initial analyses completed, data from ESCORE V&V/Re-Eval decks, data files, and project reports.
RISO	F14-6	Initial analyses completed, data from ESCORE V&V/Re-Eval decks, data files, and project reports.
RISO	F7-3	Initial analyses completed, data from ESCORE V&V/Re-Eval decks, data files, and project reports.
RISO	F8-4	Initial analyses completed, data from ESCORE V&V/Re-Eval decks, data files, and project reports.
RISO	F9-3	Initial analyses completed, data from ESCORE V&V/Re-Eval decks, data files, and project reports.
RISO	G3-2	Initial analyses completed, data from ESCORE V&V/Re-Eval decks, data files, and project reports.

Table A-1 (continued)
Instrumented and Non-Instrumented Research Rods

Case	Rod	Comment
RISO	G7-3	Initial analyses completed, data from ESCORE V&V/Re-Eval decks, data files, and project reports.
RISO	M1-3	Initial analyses completed, data from ESCORE V&V/Re-Eval decks, data files, and project reports.
RISO	M2-2B	Initial analyses completed, data from ESCORE V&V/Re-Eval decks, data files, and project reports.
RISO	M2-2C	Initial analyses completed, data from ESCORE V&V/Re-Eval decks, data files, and project reports.
RISO	M33-3	Initial analyses completed, data from ESCORE V&V/Re-Eval decks, data files, and project reports.
RISO	M61-4	Initial analyses completed, data from ESCORE V&V/Re-Eval decks, data files, and project reports.
RISO	T9-3B	Initial analyses completed, data from ESCORE V&V/Re-Eval decks, data files, and project reports.
RISO III	AN1	Initial analyses completed, data from ESCORE V&V/Re-Eval decks, data files, and project reports.
RISO III	AN10	Initial analyses completed, data from ESCORE V&V/Re-Eval decks, data files, and project reports.
RISO III	GE2	Initial analyses completed, data from ESCORE V&V/Re-Eval decks, data files, and project reports.
RISO III	GE6	Initial analyses completed, data from ESCORE V&V/Re-Eval decks, data files, and project reports.
Inter Ramp	HR2	Initial analyses completed, data from ESCORE V&V/Re-Eval decks, data files, and project reports.
Inter Ramp	HR4	Initial analyses completed, data from ESCORE V&V/Re-Eval decks, data files, and project reports.
Inter Ramp	HR5	Initial analyses completed, data from ESCORE V&V/Re-Eval decks, data files, and project reports.
Inter Ramp	LR1	Initial analyses completed, data from ESCORE V&V/Re-Eval decks, data files, and project reports.
Inter Ramp	LS2	Initial analyses completed, data from ESCORE V&V/Re-Eval decks, data files, and project reports.
Inter Ramp	TR1	Initial analyses completed, data from ESCORE V&V/Re-Eval decks, data files, and project reports.
Over Ramp	A10/1	Initial analyses completed, data from ESCORE V&V/Re-Eval decks, data files, and project reports.
Over Ramp	A10/2	Initial analyses completed, data from ESCORE V&V/Re-Eval decks, data files, and project reports.
Over Ramp	A10/3	Initial analyses completed, data from ESCORE V&V/Re-Eval decks, data files, and project reports.

Table A-1 (continued)
Instrumented and Non-Instrumented Research Rods

Case	Rod	Comment
Over Ramp	A10/4	Initial analyses completed, data from ESCORE V&V/Re-Eval decks, data files, and project reports.
Over Ramp	A20/1	Initial analyses completed, data from ESCORE V&V/Re-Eval decks, data files, and project reports.
Over Ramp	A20/3	Initial analyses completed, data from ESCORE V&V/Re-Eval decks, data files, and project reports.
Over Ramp	A20/4	Initial analyses completed, data from ESCORE V&V/Re-Eval decks, data files, and project reports.
Over Ramp	E10/1	Initial analyses completed, data from ESCORE V&V/Re-Eval decks, data files, and project reports.
Over Ramp	E10/3	Initial analyses completed, data from ESCORE V&V/Re-Eval decks, data files, and project reports.
Over Ramp	E10/4	Initial analyses completed, data from ESCORE V&V/Re-Eval decks, data files, and project reports.
Over Ramp	F20/4	Initial analyses completed, data from ESCORE V&V/Re-Eval decks, data files, and project reports.
Over Ramp	F30/1	Initial analyses completed, data from ESCORE V&V/Re-Eval decks, data files, and project reports.
Over Ramp	F30/2	Initial analyses completed, data from ESCORE V&V/Re-Eval decks, data files, and project reports.
Over Ramp	F30/4	Initial analyses completed, data from ESCORE V&V/Re-Eval decks, data files, and project reports.
Over Ramp	G20/1	Initial analyses completed, data from ESCORE V&V/Re-Eval decks, data files, and project reports.
Over Ramp	G20/2	Initial analyses completed, data from ESCORE V&V/Re-Eval decks, data files, and project reports.
Over Ramp	G20/4	Initial analyses completed, data from ESCORE V&V/Re-Eval decks, data files, and project reports.
Over Ramp	W4/2	Initial analyses completed, data from ESCORE V&V/Re-Eval decks, data files, and project reports.
Over Ramp	W4/5	Initial analyses completed, data from ESCORE V&V/Re-Eval decks, data files, and project reports.
Over Ramp	W4/6	Initial analyses completed, data from ESCORE V&V/Re-Eval decks, data files, and project reports.
Over Ramp	W5/2	Initial analyses completed, data from ESCORE V&V/Re-Eval decks, data files, and project reports.
Over Ramp	W5/3	Initial analyses completed, data from ESCORE V&V/Re-Eval decks, data files, and project reports.
Over Ramp	W5/4	Initial analyses completed, data from ESCORE V&V/Re-Eval decks, data files, and project reports.

Table A-1 (continued)
Instrumented and Non-Instrumented Research Rods

Case	Rod	Comment
Over Ramp	W5/5	Initial analyses completed, data from ESCORE V&V/Re-Eval decks, data files, and project reports.
Over Ramp	W8/3	Initial analyses completed, data from ESCORE V&V/Re-Eval decks, data files, and project reports.
Super Ramp	PK1/1	Initial analyses completed, data from ESCORE V&V/Re-Eval decks, data files, and project reports.
Super Ramp	PK1/2	Initial analyses completed, data from ESCORE V&V/Re-Eval decks, data files, and project reports.
Super Ramp	PK1/3	Initial analyses completed, data from ESCORE V&V/Re-Eval decks, data files, and project reports.
Super Ramp	PK1/4	Initial analyses completed, data from ESCORE V&V/Re-Eval decks, data files, and project reports.
Super Ramp	PK1/S	Initial analyses completed, data from ESCORE V&V/Re-Eval decks, data files, and project reports.
Super Ramp	PK2/1	Initial analyses completed, data from ESCORE V&V/Re-Eval decks, data files, and project reports.
Super Ramp	PK2/2	Initial analyses completed, data from ESCORE V&V/Re-Eval decks, data files, and project reports.
Super Ramp	PK2/3	Initial analyses completed, data from ESCORE V&V/Re-Eval decks, data files, and project reports.
Super Ramp	PK2/4	Initial analyses completed, data from ESCORE V&V/Re-Eval decks, data files, and project reports.
Super Ramp	PK2/S	Initial analyses completed, data from ESCORE V&V/Re-Eval decks, data files, and project reports.
Super Ramp	PK41GAD	Initial analyses completed, data from ESCORE V&V/Re-Eval decks, data files, and project reports.
Super Ramp	PK42GAD	Initial analyses completed, data from ESCORE V&V/Re-Eval decks, data files, and project reports.
Super Ramp	PK43GAD	Initial analyses completed, data from ESCORE V&V/Re-Eval decks, data files, and project reports.
Super Ramp	PK44GAD	Initial analyses completed, data from ESCORE V&V/Re-Eval decks, data files, and project reports.
Super Ramp	PK4/SGAD	Initial analyses completed, data from ESCORE V&V/Re-Eval decks, data files, and project reports.
Super Ramp	PK6/2	Initial analyses completed, data from ESCORE V&V/Re-Eval decks, data files, and project reports.
Super Ramp	PK6/3	Initial analyses completed, data from ESCORE V&V/Re-Eval decks, data files, and project reports.
Super Ramp	PW3/2	Initial analyses completed, data from ESCORE V&V/Re-Eval decks, data files, and project reports.

Table A-1 (continued)
Instrumented and Non-Instrumented Research Rods

Case	Rod	Comment
Super Ramp	PW3/3	Initial analyses completed, data from ESCORE V&V/Re-Eval decks, data files, and project reports.
Super Ramp	02C2	Initial analyses completed, data from ESCORE V&V/Re-Eval decks, data files, and project reports.
Super Ramp	02C4	Initial analyses completed, data from ESCORE V&V/Re-Eval decks, data files, and project reports.
Super Ramp	03C4	Initial analyses completed, data from ESCORE V&V/Re-Eval decks, data files, and project reports.
Super Ramp	13C2	Initial analyses completed, data from ESCORE V&V/Re-Eval decks, data files, and project reports.
Super Ramp	13C3	Initial analyses completed, data from ESCORE V&V/Re-Eval decks, data files, and project reports.
OPPD/DOE	KJE076	Initial analyses completed, data from ESCORE V&V/Re-Eval decks, data files, and project reports.
OPPD/DOE	KJE085	Initial analyses completed, data from ESCORE V&V/Re-Eval decks, data files, and project reports.
OPPD/DOE	KJD125	Initial analyses completed, data from ESCORE V&V/Re-Eval decks, data files, and project reports.
OPPD/DOE	KJD157	Initial analyses completed, data from ESCORE V&V/Re-Eval decks, data files, and project reports.
OPPD/DOE	KJN037	Initial analyses completed, data from ESCORE V&V/Re-Eval decks, data files, and project reports.
OPPD/DOE	KJN052	Initial analyses completed, data from ESCORE V&V/Re-Eval decks, data files, and project reports.
OPPD/DOE	KJN064	Initial analyses completed, data from ESCORE V&V/Re-Eval decks, data files, and project reports.
OPPD/DOE	KJM098	Initial analyses completed, data from ESCORE V&V/Re-Eval decks, data files, and project reports.
OPPD/DOE	KKM090	Initial analyses completed, data from ESCORE V&V/Re-Eval decks, data files, and project reports.
OPPD/DOE	KKM094	Initial analyses completed, data from ESCORE V&V/Re-Eval decks, data files, and project reports.
OPPD/DOE	KKM095	Initial analyses completed, data from ESCORE V&V/Re-Eval decks, data files, and project reports.
OPPD/DOE	KKM098	Initial analyses completed, data from ESCORE V&V/Re-Eval decks, data files, and project reports.
Petten/DOE	1/23	Initial analyses completed, data from ESCORE V&V/Re-Eval decks, data files, and project reports.
Petten/DOE	1/24	Initial analyses completed, data from ESCORE V&V/Re-Eval decks, data files, and project reports.

Table A-1 (continued)
Instrumented and Non-Instrumented Research Rods

Case	Rod	Comment
Petten/DOE	V30/2	Initial analyses completed, data from ESCORE V&V/Re-Eval decks, data files, and project reports.
Petten/DOE	V30/5	Initial analyses completed, data from ESCORE V&V/Re-Eval decks, data files, and project reports.
Petten/DOE	V40/1	Initial analyses completed, data from ESCORE V&V/Re-Eval decks, data files, and project reports.
Petten/DOE	V40/2	Initial analyses completed, data from ESCORE V&V/Re-Eval decks, data files, and project reports.
Petten/DOE	V40/3	Initial analyses completed, data from ESCORE V&V/Re-Eval decks, data files, and project reports.
Petten/DOE	V40/4	Initial analyses completed, data from ESCORE V&V/Re-Eval decks, data files, and project reports.
Petten/DOE	V40/5	Initial analyses completed, data from ESCORE V&V/Re-Eval decks, data files, and project reports.
BR-3	11	Initial analyses completed, data from ESCORE V&V/Re-Eval decks, data files, and project reports.
BR-3	24	Initial analyses completed, data from ESCORE V&V/Re-Eval decks, data files, and project reports.
BR-3	28	Initial analyses completed, data from ESCORE V&V/Re-Eval decks, data files, and project reports.
BR-3	30	Initial analyses completed, data from ESCORE V&V/Re-Eval decks, data files, and project reports.
BR-3	36	Initial analyses completed, data from ESCORE V&V/Re-Eval decks, data files, and project reports.
Zorita	328	Initial analyses completed, data from ESCORE V&V/Re-Eval decks, data files, and project reports.
Zorita	331	Initial analyses completed, data from ESCORE V&V/Re-Eval decks, data files, and project reports.
Zorita	332	Initial analyses completed, data from ESCORE V&V/Re-Eval decks, data files, and project reports.
Zorita	334	Initial analyses completed, data from ESCORE V&V/Re-Eval decks, data files, and project reports.
Zorita	335	Initial analyses completed, data from ESCORE V&V/Re-Eval decks, data files, and project reports.
Zorita	344	Data from ESCORE V&V/Re-Eval decks, data files, and project reports. Error in conversion under review.
Zorita	384	Data from ESCORE V&V/Re-Eval decks, data files, and project reports. Error in conversion under review.
Zorita	385	Data from ESCORE V&V/Re-Eval decks, data files, and project reports. Error in conversion under review.
Zorita	386	Data from ESCORE V&V/Re-Eval decks, data files, and project reports. Error in conversion under review.

Table A-2
Commercial Rods

Case	Rod	Comment
Limerick	yj1433-e9	Preliminary input deck completed, review underway, from vendor/utility data
Limerick	yj1433-f9	Preliminary input deck completed, review underway, from vendor/utility data
Limerick	yj1433-g1	Preliminary input deck completed, review underway, from vendor/utility data
Limerick	yj1433-j3	Preliminary input deck completed, review underway, from vendor/utility data
Limerick	yj1433-j4	Preliminary input deck completed, review underway, from vendor/utility data
Limerick	yj1433-j7	Preliminary input deck completed, review underway, from vendor/utility data
HB Robinson	RA18229	Preliminary input deck completed, review underway, from vendor/utility data
HB Robinson	RA18293	Preliminary input deck completed, review underway, from vendor/utility data
HB Robinson	RA18311	Preliminary input deck completed, review underway, from vendor/utility data
HB Robinson	RA18308	Preliminary input deck completed, review underway, from vendor/utility data
HB Robinson	RA18300	Preliminary input deck completed, review underway, from vendor/utility data
HB Robinson	RA19867	Preliminary input deck completed, review underway, from vendor/utility data
HB Robinson	RA19865	Preliminary input deck completed, review underway, from vendor/utility data
HB Robinson	RA18235	Preliminary input deck completed, review underway, from vendor/utility data
HB Robinson	RA18302	Preliminary input deck completed, review underway, from vendor/utility data
HB Robinson	BL219926	Preliminary input deck completed, review underway, from vendor/utility data
HB Robinson	BG02438	Preliminary input deck completed, review underway, from vendor/utility data
HB Robinson	RA110889	Preliminary input deck completed, review underway, from vendor/utility data
GG LTA-901	HA001301	Preliminary input deck completed, review underway, from vendor/utility data
GG LTA-901	HA001403	Preliminary input deck completed, review underway, from vendor/utility data

Table A-2 (continued)
Commercial Rods

Case	Rod	Comment
GG LTA-901	HA001503	Preliminary input deck completed, review underway, from vendor/utility data
GG LTA-901	HA001601	Preliminary input deck completed, review underway, from vendor/utility data
GG LTA-901	HA101701	Preliminary input deck completed, review underway, from vendor/utility data
GG LTA-901	HA101702	Preliminary input deck completed, review underway, from vendor/utility data
GG LTA-901	HA101801	Preliminary input deck completed, review underway, from vendor/utility data
GG LTA-901	HA101802	Preliminary input deck completed, review underway, from vendor/utility data
GG LTA-901	HA101901	Preliminary input deck completed, review underway, from vendor/utility data
GG LTA-901	HA101902	Preliminary input deck completed, review underway, from vendor/utility data
GG LTA-901	HA102103	Preliminary input deck completed, review underway, from vendor/utility data
GG LTA-901	HA102104	Preliminary input deck completed, review underway, from vendor/utility data
GG LTA-901	HA102201	Preliminary input deck completed, review underway, from vendor/utility data
GG LTA-901	HA102401	Preliminary input deck completed, review underway, from vendor/utility data
GG LTA-901	HA102402	Preliminary input deck completed, review underway, from vendor/utility data
GG LTA-901	HA102402	Preliminary input deck completed, review underway, from vendor/utility data
GG LTA-901	HA302001	Preliminary input deck completed, review underway, from vendor/utility data
GG LTA-901	HA302002	Preliminary input deck completed, review underway, from vendor/utility data
GG LTA-901	HA302004	Preliminary input deck completed, review underway, from vendor/utility data
GG LTA-901	HA302303	Preliminary input deck completed, review underway, from vendor/utility data
Ft. Calhoun/CE	KJD-125	Initial analyses completed, data from ESCORE V&V/Re-Eval decks, data files, and project reports.

Table A-2 (continued)
Commercial Rods

Case	Rod	Comment
Ft. Calhoun/CE	KJD-076	Initial analyses completed, data from ESCORE V&V/Re-Eval decks, data files, and project reports.
Main Yankee	JBY097	Initial analyses completed, data from ESCORE V&V/Re-Eval decks, data files, and project reports.
Oconee	15159 A1	Initial analyses completed, data from ESCORE V&V/Re-Eval decks, data files, and project reports.
Peach Bottom	F3/C6	Initial analyses completed, data from ESCORE V&V/Re-Eval decks, data files, and project reports.
Peach Bottom 3	DJD-0220 C3	Initial analyses completed, data from ESCORE V&V/Re-Eval decks, data files, and project reports.
Peach Bottom 3	DJD-0224 F4	Initial analyses completed, data from ESCORE V&V/Re-Eval decks, data files, and project reports.
Quad Cities 1	G7	Initial analyses completed, data from ESCORE V&V/Re-Eval decks, data files, and project reports.
Dresden 2	DRS220a1	Preliminary input deck completed, review underway, from vendor/utility data
Dresden 2	DRS220a4	Preliminary input deck completed, review underway, from vendor/utility data
Dresden 2	DRS220a5	Preliminary input deck completed, review underway, from vendor/utility data
Dresden 2	DRS220a7	Preliminary input deck completed, review underway, from vendor/utility data
Dresden 2	DRS220b2	Preliminary input deck completed, review underway, from vendor/utility data
Dresden 2	DRS220b7	Preliminary input deck completed, review underway, from vendor/utility data
Dresden 2	DRS220b8	Preliminary input deck completed, review underway, from vendor/utility data
Dresden 2	DRS220c4	Preliminary input deck completed, review underway, from vendor/utility data
Dresden 2	DRS220d1	Preliminary input deck completed, review underway, from vendor/utility data
Dresden 2	DRS220d3	Preliminary input deck completed, review underway, from vendor/utility data

Table A-2 (continued)
Commercial Rods

Case	Rod	Comment
Dresden 2	DRS220d4	Preliminary input deck completed, review underway, from vendor/utility data
Dresden 2	DRS220d7	Preliminary input deck completed, review underway, from vendor/utility data
Dresden 2	DRS220e1	Preliminary input deck completed, review underway, from vendor/utility data
Dresden 2	DRS220e4	Preliminary input deck completed, review underway, from vendor/utility data
Dresden 2	DRS220f7	Preliminary input deck completed, review underway, from vendor/utility data
Dresden 2	DRS220g1	Preliminary input deck completed, review underway, from vendor/utility data
Dresden 2	DRS220g2	Preliminary input deck completed, review underway, from vendor/utility data
Dresden 2	DRS220g4	Preliminary input deck completed, review underway, from vendor/utility data
Dresden 2	DRS220g6	Preliminary input deck completed, review underway, from vendor/utility data
Dresden 2	DRS220g8	Preliminary input deck completed, review underway, from vendor/utility data
Dresden 2	DRS220h2	Preliminary input deck completed, review underway, from vendor/utility data
Dresden 2	DRS220h7	Preliminary input deck completed, review underway, from vendor/utility data
Dresden 2	DRS220h8	Preliminary input deck completed, review underway, from vendor/utility data
Dresden 2	DRS228a1	Preliminary input deck completed, review underway, from vendor/utility data
Dresden 2	DRS228a3	Preliminary input deck completed, review underway, from vendor/utility data
Dresden 2	DRS228a5	Preliminary input deck completed, review underway, from vendor/utility data
Dresden 2	DRS228a6	Preliminary input deck completed, review underway, from vendor/utility data
Dresden 2	DRS228a8	Preliminary input deck completed, review underway, from vendor/utility data
Dresden 2	DRS228b1	Preliminary input deck completed, review underway, from vendor/utility data
Dresden 2	DRS228b3	Preliminary input deck completed, review underway, from vendor/utility data

Table A-2 (continued)
Commercial Rods

Case	Rod	Comment
Dresden 2	DRS228b9	Preliminary input deck completed, review underway, from vendor/utility data
Dresden 2	DRS228c2	Preliminary input deck completed, review underway, from vendor/utility data
Dresden 2	DRS228c3	Preliminary input deck completed, review underway, from vendor/utility data
Dresden 2	DRS228c4	Preliminary input deck completed, review underway, from vendor/utility data
Dresden 2	DRS228d3	Preliminary input deck completed, review underway, from vendor/utility data
Dresden 2	DRS228d4	Preliminary input deck completed, review underway, from vendor/utility data
Dresden 2	DRS228d9	Preliminary input deck completed, review underway, from vendor/utility data
Dresden 2	DRS228e1	Preliminary input deck completed, review underway, from vendor/utility data
Dresden 2	DRS228e8	Preliminary input deck completed, review underway, from vendor/utility data
Dresden 2	DRS228f1	Preliminary input deck completed, review underway, from vendor/utility data
Dresden 2	DRS228f9	Preliminary input deck completed, review underway, from vendor/utility data
Dresden 2	DRS228g7	Preliminary input deck completed, review underway, from vendor/utility data
Dresden 2	DRS228h1	Preliminary input deck completed, review underway, from vendor/utility data
Dresden 2	DRS228h2	Preliminary input deck completed, review underway, from vendor/utility data
Dresden 2	DRS228h5	Preliminary input deck completed, review underway, from vendor/utility data
Dresden 2	DRS228k2	Preliminary input deck completed, review underway, from vendor/utility data
Dresden 2	DRS228k4	Preliminary input deck completed, review underway, from vendor/utility data
Dresden 2	DRS228k6	Preliminary input deck completed, review underway, from vendor/utility data
Dresden 2	DRS228k9	Preliminary input deck completed, review underway, from vendor/utility data

Table A-3
Instrumented and Non-Instrumented Research Rods Under Preparation

Case	Comment
IFA 429.1	Power history and measurement data extraction from TFDB completed. Working data compression issues.
IFA 429.2	Power history and measurement data extraction from TFDB completed. Working data compression issues.
IFA 429.3	Power history and measurement data extraction from TFDB completed. Working data compression issues.
IFA 429.4	Power history and measurement data extraction from TFDB completed. Working data compression issues.
IFA 429.5	Power history and measurement data extraction from TFDB completed. Working data compression issues.
IFA 429.6	Power history and measurement data extraction from TFDB completed. Working data compression issues.
IFA 429.7	Power history and measurement data extraction from TFDB completed. Working data compression issues.
IFA 431	Power history and measurement data extraction from TFDB completed. Working data compression issues.
IFA 432.1	Power history and measurement data extraction from TFDB completed. Working data compression issues.
IFA 432.2	Power history and measurement data extraction from TFDB completed. Working data compression issues.
IFA 432.3	Power history and measurement data extraction from TFDB completed. Working data compression issues.
IFA 432.4	Power history and measurement data extraction from TFDB completed. Working data compression issues.
IFA 508.1	Power history and measurement data extraction from TFDB completed. Working data compression issues.
IFA 513.1	Power history and measurement data extraction from TFDB completed. Working data compression issues.
IFA 513.2	Power history and measurement data extraction from TFDB completed. Working data compression issues.
IFA 513.3	Power history and measurement data extraction from TFDB completed. Working data compression issues.
IFA 513.4	Power history and measurement data extraction from TFDB completed. Working data compression issues.

Table A-4
Commercial Rods Under Preparation

Case	Comment
Calvert Cliffs	13 Rods from the PROTOTYPE Program conducted at Calvert Cliffs-1. Power history and rod data being compiled. Decks under development.
Grohnde	All power history files have been converted for input into FALCON from vendor/utility data. Input decks under development. Total of 63 rods available.
Gösgen	Power history files have been compiled. Input decks under development. Total of 17 rods available.

B
APPENDIX B

The following pages contain the FALCON V&V database fuel parameter, design data, and power history request form. The form is broken down into five tables:

1. Fuel pellet material, dimensional and property data and parameters
2. Cladding material, dimensional and property data and parameters
3. Overall fuel rod design parameters
4. Thermal hydraulic parameters
5. Distribution and history data
    a. Power history and axial shape
    b. Iron particle size
    c. Coolant lithium history

Appendix B

Fuel Pellet	English Units	Value	Metric Units	Value	Default	Priority	Comments
Material						Required	UO_2, UO_2-Gd_2O_3, or MOX
Gd_2O_3	wt% Gd_2O_3		wt% Gd_2O_3			Optional	Required if Gd
MOX Pu Fraction	wt% Pu		wt% Pu			Optional	Required if MOX
^{235}U Enrichment							
Enrichment Zones	n/a		n/a			Required	Number of enrichment zones
Enriched Pellet	wt% ^{235}U		wt% ^{235}U			Required	
Gd_2O_3 Pellet	wt% ^{235}U		wt% ^{235}U			Optional	Required if Gd
MOX Pellet	wt% ^{235}U		wt% ^{235}U			Optional	Required if MOX
Natural Pellet	wt% ^{235}U		wt% ^{235}U		0.7	Optional	Default value used if not specified
Dimensions							
Enriched Pellet Inner Diameter	in		mm			Required	Required if annular pellet
Enriched Pellet Outer Diameter	in		mm			Required	
Enriched Pellet Length	in		mm			Required	
Natural Pellet Inner Diameter	in		mm			Optional	Default to enriched pellet dimensions if not specified
Natural Pellet Outer Diameter	in		mm			Optional	Default to enriched pellet dimensions if not specified
Natural Pellet Length	in		mm			Optional	Default to enriched pellet dimensions if not specified
Characteristics/Properties							
Theoretical Density	%TD		%TD			Required	
Open Porosity	%		%			Required	
Dish Volume	in^3 or %		m^3 or %		0.0	Optional	Specify total volume with units or dimensions below
Diameter	in		mm		0.0	Optional	
Depth	in		mm		0.0	Optional	
Chamfer Volume	in^3 or %		m^3 or %		0.0	Optional	Specify total volume with units or dimensions below
Width	in		mm		0.0	Optional	
Length	in		mm		0.0	Optional	
Angle	degrees		degrees		0.0	Optional	
Surface Roughness	μin		μm		1.6	Optional	Default value [μm] used if not specified
Grain Size	mils		μm		10.0	Optional	Default value [μm] used if not specified

Cladding	English Units	Value	Metric Units	Value	Default	Priority	Comments
Material							
Cladding Type	n/a		n/a			Required	Primary cladding composition: Zr-2, Zr-4, Zirlo, M5, etc.
Barrier Cladding (BWR)	n/a		n/a			Required	
Barrier Composition	n/a		n/a		Zr	Optional	Required if barrier cladding
Duplex Cladding (PWR)	n/a		n/a			Required	
Duplex Layer Composition	n/a		n/a			Optional	Required if duplex cladding
Dimensions							
Inner Diameter	in		mm			Required	Specify either thickness or inner diameter
Wall thickness	in		mm			Optional	
Outer Diameter	in		mm			Required	
Cladding Liner Thickness	in		mm			Optional	Required if barrier cladding
Duplex Layer Thickness	in		mm			Optional	Required if duplex cladding
Characteristics/Properties							
Inner Diam Surface Roughness	μin		μm		1.6	Optional	Default value [μm] used if not specified
Annealing Parameter						Optional	Can use cold work
Cladding Cold Work	%		%			Optional	Can use typical values or yield stress and corresponding temperature
Unirradiated 0.2% Yield Stress	ksi, ^{o}F		MPa, ^{o}C				Stress and corresponding temperature
Ultimate Yield Strength	ksi, ^{o}F		MPa, ^{o}C				Strength and corresponding temperature
Oxygen Concentration	lbm O_2/lbm Zr		kg O_2/kg Zr			Optional	
Tin Content (PWR)	wt%		wt%			Optional	For PWR corrosion modeling
Iron Particle Size Distr. (PWR)	μm fractional distribution					Optional	For PWR corrosion modeling, see comments below

Fuel Rod	English Units	Value	Metric Units	Value	Default	Priority	Comments
Overall Length	in		mm			Required	
Enriched Fuel Column Height	in		mm			Required	
Top Blanket Height	in		mm		150.0	Optional	Default value [mm] used if not specified
Bottom Blanket Height	in		mm		150.0	Optional	Default value [mm] used if not specified
Upper Plenum Length	in		mm			Optional	Can use typical values
Lower Plenum Length	in		mm			Optional	Can use typical values
Empty Plenum Volume	in^3		cm^3			Optional	Can use typical values
Plenum Spring Volume	in^3		cm^3			Optional	
Spring Vol/Plenum Vol Ratio	%		%		10.0	Optional	Default is 10% of plenum volume
Plenum Spring Rate	psi		N/m		3500.0	Optional	Default value [N/m] used if not specified
Upper End Plug Length	in		mm			Optional	
Lower End Plug Length	in		mm			Optional	
Fill Gas Composition	%		%		100% He	Optional	Required if not He
Internal Fill Gas Pressure	psi		MPa			Required	
Corresponding Fill Gas Temp	^{o}F		^{o}C			Required	Must correspond to fill gas pressure

Appendix B

Thermal Hydraulic	English Units	Value	Metric Units	Value	Default	Priority	Comments
Initial Inlet Coolant Pressure	psi		MPa			Required	
Coolant Mass Flux Rate	lbm/hr-ft^2		kg/s-m^2			Required	
Coolant Inlet Temperature	^{o}F		^{o}C			Required	
Coolant Oulet Temperature	^{o}F		^{o}C			Optional	
Fuel Rod Pitch	in		mm			Required	Specify either pitch or hydraulic diameter
Hydraulic Diameter	in		mm			Optional	Specify either pitch or hydraulic diameter
Coolant Li Content Hist (PWR)	ppm		ppm			Optional	For corrosion modeling, see comments below for format

Distribution and History Data	Comments
Power History and Axial Shape	There are several methods for submission of power history and axial shape data. The options are listed below in order of preference. Option 1: Electronic ASCII files of average rod power [kw/m or kw/ft] and axial shape [normalized versus elevation measured from an axial reference point] as functions of time. Option 2: Electronic ASCII files of core-follow data dumps from neutronics codes, i.e. CASMO/SIMULATE, etc. Option 3: Hard copy print outs of data formatted per Option 1 or 2.
Iron Particle Size Distribution (PWR)	Electronic ASCII data files or hardcopies of arrays of distribution fraction (of total) versus particle size (μm)
Coolant Li Content History (PWR)	Electronic ASCII data files or hardcopies of arrays of lithium content (ppm) as a function of time

WARNING: This Document contains information classified under U.S. Export Control regulations as restricted from export outside the United States. You are under an obligation to ensure that you have a legal right to obtain access to this information and to ensure that you obtain an export license prior to any re-export of this information. Special restrictions apply to access by anyone that is not a United States citizen or a Permanent United States resident. For further information regarding your obligations, please see the information contained below in the section titled 'Export Control Restrictions."

Export Control Restrictions

Access to and use of EPRI Intellectual Property is granted with the specific understanding and requirement that responsibility for ensuring full compliance with all applicable U.S. and foreign export laws and regulations is being undertaken by you and your company. This includes an obligation to ensure that any individual receiving access hereunder who is not a U.S. citizen or permanent U.S. resident is permitted access under applicable U.S. and foreign export laws and regulations. In the event you are uncertain whether you or your company may lawfully obtain access to this EPRI Intellectual Property, you acknowledge that it is your obligation to consult with your company's legal counsel to determine whether this access is lawful. Although EPRI may make available on a case by case basis an informal assessment of the applicable U.S. export classification for specific EPRI Intellectual Property, you and your company acknowledge that this assessment is solely for informational purposes and not for reliance purposes. You and your company acknowledge that it is still the obligation of you and your company to make your own assessment of the applicable U.S. export classification and ensure compliance accordingly. You and your company understand and acknowledge your obligations to make a prompt report to EPRI and the appropriate authorities regarding any access to or use of EPRI Intellectual Property hereunder that may be in violation of applicable U.S. or foreign export laws or regulations.

About EPRI

EPRI creates science and technology solutions for the global energy and energy services industry. U.S. electric utilities established the Electric Power Research Institute in 1973 as a nonprofit research consortium for the benefit of utility members, their customers, and society. Now known simply as EPRI, the company provides a wide range of innovative products and services to more than 1000 energy-related organizations in 40 countries. EPRI's multidisciplinary team of scientists and engineers draws on a worldwide network of technical and business expertise to help solve today's toughest energy and environmental problems.

EPRI. Electrify the World

Program: 1002866

Nuclear Power

EPRI • 3412 Hillview Avenue, Palo Alto, California 94304 • PO Box 10412, Palo Alto, California 94303 • USA
800.313.3774 • 650.855.2121 • askepri@epri.com • www.epri.com